Figure 8 FKBP8 interacts with NS5A and Hsp90 via different sites in the TPR domain and participates in HCV replication. (**A**) Flag-FKBP8 was coexpressed with HA-Hsp90 or HA-Hsp90ΔMEEDV lacking the C-terminal MEEDV residues and was immunoprecipitated by anti-HA or anti-Flag antibody. Precipitates were analyzed by Western blotting. (**B**) Sequence alignment of TPR domains of FKBP8, FKBP52, and CypD. The two bold characters (K and R) indicate amino-acid residues substituted to Ala in FKBP8TPRmut. (**C**) Flag-FKBP8 or Flag-FKBP8TPRmut substituted Lys^{307} and Arg^{311} to Ala was coexpressed with HA-Hsp90 (left) or HA-NS5A (right) in 293T cells, and was immunoprecipitated by anti-HA or anti-Flag antibody. Precipitates were analyzed by Western blotting. (**D**) Flag-FKBP8, Flag-FKBP8TPRmut, or empty plasmid was transfected into the replicon cells and HCV RNA was determined by real-time PCR after 48 h transfection. Relative replication was expressed as % increase after being normalized with the expression of β-actin mRNA. (**E**) The effect of geldanamycin on HCV RNA replication. HCV replicon cells (9–13 cells) were treated with 1, 3, 10, and 30 nM of geldanamycin and after 24 h treatment, HCV RNA replication was determined by real-time PCR. Relative replication was expressed as % replication after standardized by the expression of β-actin (closed circles). Cell viabilities were determined by trypan blue staining (closed triangles). (**F**) The effect of geldanamycin on the expression of NS5A and FKBP8. The replicon cells were examined by immunoblotting after treatment with various concentrations of geldanamycin. The data shown in each panel are representative of three independent experiments.

(Watashi *et al*, 2003, 2005). These results support the notion that FK506 preferentially binds to FKBP members other than FKBP8 *in vivo*, and that it does not participate in the inhibition of HCV replication.

Cellular and viral chaperones are implicated in the processing of viral proteins and viral assembly (Maggioni and Braakman, 2005; Mayer, 2005). The NS2 protein of bovine viral diarrhea virus (BVDV), a member of the *Flaviviridae* family as is HCV, exhibits autoprotease activity that leads to cleavage at the NS2 and NS3 junction (Lackner *et al*, 2005). A noncytopathogenic strain of BVDV is unable to cleave the NS2/3 junction in the absence of the interaction of a molecular chaperone, J-domain protein interacting with viral protein (Jiv); these previous findings suggest that Jiv is

necessary for the replication of a noncytopathogenic strain of BVDV and is involved in the establishment of persistent infection (Lackner *et al*, 2005). Furthermore, FKBP52, which shares a high homology with FKBP8, was shown to regulate replication of adeno-associated virus type 2 by interacting with viral DNA (Qing *et al*, 2001). In this study, we demonstrated that HCV NS5A binds to FKBP8 and forms a complex with Hsp90. FKBP8 could directly bind to NS5A domain I *in vitro* (Supplementary Figure 1), suggesting that Hsp90 is not required for interaction between NS5A and FKBP8. FKBP52 forms a homodimer, binds to Hsp90 through TPR domain, and regulates chaperone activity of Hsp90 (Silverstein *et al*, 1999; Scheufler *et al*, 2000; Wu *et al*, 2004). FKBP8 may act as cochaperone of Hsp90 to regulate

HCV genome replication by interaction with NS5A. Hsp90 is a molecular chaperone that is highly expressed in most cell types in various organisms (Neckers, 2002). Here, Hsp90 was found to be able to bind to FKBP8 and form a complex with HCV NS5A. The suppression of NS5A, but not that of FKBP8, was observed in replicon cells treated with geldanamycin, thus suggesting that Hsp90 regulates the replication of HCV RNA via the interaction with FKBP8. It is well known that several host proteins such as VAPs and FBL2 interact with the HCV replication complex and regulate HCV RNA replication (Evans et al, 2004; Gao et al, 2004; Hamamoto et al, 2005; Wang et al, 2005). The TPR domain of FKBP8 is composed of 220 amino acids and is too long to determine the critical residues responsible for interaction with NS5A. Therefore, we tried to make a chimeric mutant carrying the TPR of FKBP52 to determine the critical amino-acid residues for binding to NS5A in FKBP8. However, expression of a chimeric FKBP8 possessing TPR of FKBP52 was much lower than the native form, suggesting that TPR domain is critical for stability and conformation of FKBP8. Amino-acid residues responsible for the binding to NS5A must be different from the two-carboxylate positions responsible for Hsp90 binding and locate within the TPR domain. The ternary complex consists of NS5A, FKBP8 and Hsp90 may be involved in the replication of HCV. FKBP52 possesses PPIase activity and chaperone activity in domain I (amino acids 1–148) and domain 3 (TPR domain, amino acids 264–400), respectively (Pirkl et al, 2001). Therefore, it is reasonable to speculate that the TPR domain is responsible for the chaperone activity of FKBP8, and that the FKBP8 and NS5A complex transports Hsp90 to the appropriate clients, including viral and host proteins, which in turn leads to the stabilization of the replication complex and the enhancement of HCV RNA replication.

In this study, we identified human FKBP8 as a binding partner of HCV NS5A. Our results suggest that the interaction between FKBP8 and HCV NS5A is essential for HCV replication. The NS5A protein forms a complex with FKBP8 and Hsp90, and an inhibitor of Hsp90 was shown to reduce the efficiency of HCV replication. The elucidation of the molecular mechanisms underlying the formation of the NS5A/FKBP8/Hsp90 complex may lead to the development of new therapeutics for chronic hepatitis C.

Materials and methods

Yeast two-hybrid assays
Screening for the gene-encoding host protein that interacts with HCV NS5A was performed with a yeast two-hybrid system, Matchmaker two-hybrid system 3 (Clontech, Palo Alto, CA), according to the manufacturer's protocol. Human fetal brain and liver libraries were purchased from Clontech. The cDNA of NS5A-encoding amino acids 1973–2419 of an HCV polyprotein of the J1 strain (genotype 1b) (Aizaki et al, 1998) was amplified by PCR and was cloned into the pGBKT7 vector (Clontech) (Tu et al, 1999; Hamamoto et al, 2005).

Plasmids
DNA fragments encoding NS5A were amplified from HCV genotype 1b strains J1 and Con1 (provided by Dr Bartenschlager), genotype 1a strain H77C (provided by Dr Bukh), and genotype 2a strain JFH-1 (provided by Dr Wakita) by PCR using Pfu turbo DNA polymerase (Stratagene, La Jolla, CA). The fragments were cloned into pCAGGs-PUR/N-HA, in which the sequence encoding an HA tag is inserted at the 5′-terminus of the cloning site of pCAGGs-PUR (Niwa et al, 1991). The DNA fragment encoding human FKBP8 was amplified from the total cDNA of Huh7 cells by PCR, and this

fragment was introduced into pEF-FLAG pGBK puro (Huang et al, 1997), pCAGGs-PUR/NHA, pcDNA3.1-N-HA (Tu et al, 1999; Hamamoto et al, 2005), and pcDNA3.1-N-EE, in which an Glu-Glu (EE) tag is inserted in the 5′-terminus of the cloning site of pcDNA3.1 (+) (Invitrogen, Carlsbad, CA). The DNA fragments encoding human Hsp90, FKBP52, and CypD were amplified from a human fetal brain library (Clontech) by PCR, and were introduced into pcDNA3.1-N-HA. The genes encoding the deletion mutants of human FKBP8 were amplified and cloned into pCAGGs-PUR/NHA. The gene encoding an FKBP8 mutant replaced Lys[307] and Arg[311] with Ala, designated as FKBP8TPRmut, was generated by the method of splicing by overlap extension and introduced into pEF-Flag pGBKpuro. The gene encoding an Hsp90 mutant lacking the C-terminal MEEVD motif of Hsp90, designated as Hsp90ΔMEEVD, was amplified and cloned into pcDNA3.1-N-HA. All PCR products were confirmed by sequencing by an ABI PRSM 310 genetic analyzer (Applied Biosystems, Tokyo, Japan).

Cell lines
Human embryonic kidney 293T cells and the human hepatoma cell lines Huh7 and FLC-4 were maintained in Dulbecco's modified Eagle's medium (DMEM) (Sigma, St Louis, MO) containing 10% fetal calf serum (FCS), whereas the Huh 9-13 cell line, which possesses an HCV subgenomic replicon (Lohmann et al, 1999), was cultured in DMEM supplemented with 10% FCS and 1 mg/ml G418. All cells were cultured at 37°C in a humidified atmosphere with 5% CO_2.

Antibodies
Mouse monoclonal antibodies to the HA and EE tags were purchased from Covance (Richmond, CA). Anti-Flag mouse antibody M2, horseradish peroxidase-conjugated M2 antibody, and anti-β-actin mouse monoclonal antibody were purchased from Sigma. Mouse monoclonal antibody to NS5A was from Austral Biologicals (San Ramon, CA). Mouse monoclonal antibodies to NS4B and NS5B have been described previously (Kashiwagi et al, 2002). Rabbit polyclonal antibody to NS5A was prepared as described previously (Hamamoto et al, 2005). Rabbit polyclonal antibody to thioredoxin was described previously (Moriishi et al, 1999).

Transfection, immunoblotting, and immunoprecipitation
The transfection and immunoprecipitation test were carried out by a previously described method (Hamamoto et al, 2005). The immunoprecipitates boiled in the loading buffer were subjected to 12.5% SDS–PAGE. The proteins were transferred to polyvinylidene difluoride membranes (Millipore, Bedford, MA) and were reacted with the appropriate antibodies. The immune complexes were visualized with Super Signal West Femto substrate (Pierce, Rockford, IL) and they were detected by an LAS-3000 image analyzer system (Fujifilm, Tokyo, Japan). The density of protein band was determined by using IMAGE-PRO PLUS 5.1 software (Media Cybernetics, Silver Springs, MD).

Gene silencing by siRNA
The siRNA targeted to FKBP8, Target-1: 5′-GAGUGGCUGGACAUUC UGG-3′, and negative control siRNA, that is, siCONTROL Non-Targeting siRNA-2, were purchased from Dharmacon (Lafayette, CO). Target-2, 5′-UCCCAUGGAAGUGGCUGUU-3′, and Target-3, 5′-GACAACAUCAAGGCUCUCU-3′ were purchased from Qiagen (Tokyo, Japan). The Huh7 cells harboring a subgenomic HCV replicon grown on six-well plates were transfected with 80 or 160 nM of siRNA with siFECTOR (B-Bridge International, Sunnyvale, CA). The cells were grown in DMEM containing 10% FCS and were then harvested at 48 or 72 h post-transfection.

Real-time PCR
Total RNA was prepared from cell lines by using RNeasy mini kit (Qiagen). First-strand cDNA was synthesized by using a first-strand cDNA synthesis kit (Amersham Pharmacia Biotech, Franklin Lakes, NJ) and random primers. Each cDNA was estimated by Platinum SYBR Green qPCR SuperMix UDG (Invitrogen) according to the manufacturer's protocol. Fluorescent signals were analyzed by an ABI PRISM 7000 (Applied Biosystems). The HCV NS5A, human β-actin, and human FKBP8 genes were amplified using the primer pairs of 5′-AGTCAGTTGTCTGCGCTTTC-3′ and 5′-CGGGGAATTTCCTGGTCTTC-3′,

5'-TGGAGTCCTGTGGCATCCACGAAACTACCTTCAACTC-3'
and 5'-CGGACTCGTCATACTCCTGCTTGCTGATCCACATC-3',
and 5'-GGCTGTTGAGGAAGAAGACG-3'
and 5'-CTTGGAGTCAGCAGTGACCA-3', respectively. The FKBP8 primers are located at different exons in order to prevent the false-positive amplification of contaminated genomic DNA. The values of the HCV genome and FKBP8 mRNA were normalized with those of β-actin mRNA. Each PCR product was detected as a single band of the correct size upon agarose gel electrophoresis (data not shown).

Establishment of cell lines expressing an siRNA-resistant FKBP8 mutant and knockdown FKBP8 expression

A, G, and T at nucleotides 273, 276, and 288 from the 5' end of the open-reading frame of human FKBP8 were replaced with G, A, and C, respectively, according to a splicing method achieved by overlap extension; these silent mutations were then cloned into pEF-Flag pGBKpuro. The resulting plasmid encoding a mutant FKBP8 resistant to knockdown by siRNA was transfected into Huh7 cells harboring the HCV RNA replicon. The culture medium was replaced with DMEM supplemented with 10% FCS and 2 μg/ml of puromycin (Nakarai Tesque, Tokyo, Japan) at 24 h post-transfection, and the cells were cultured for 7 days. The surviving cells were used for the FKBP8 knockdown experiments. The shRNAs targeted to FKBP8, the target sequences of which were 5'-GATCCGCTGGAACCTTCCA ACAAGTTCAAGAGACTTGTTGGAAGGTTCCAGCTTA-3', and 5'-A GCTTAAGCTGGAACCTTCCAACAAGTCTCTTGAACTTGTTGGAAGG TTCCAGCG-3', were annealed and introduced between the BamHI and HindIII sites of pSilencer™ 2.1-U6 hygro (Ambion, Austin, TX) according to the manufacturer's protocol. An HCV replicon cell line cured with IFN-α was transfected with 5 μg of the plasmid by electroporation. The culture medium was replaced with DMEM supplemented with 10% FCS and 500 μg/ml of Hygromycin B (Wako, Tokyo, Japan) at 24 h post-transfection. The remaining cells were re-seeded in 98-well plates and cloned for the colony formation and transient replication assays.

Colony formation assay

The plasmid pFK-I$_{389}$ neo/NS3-3'/NK5.1 (Pietschmann et al, 2002) was obtained from R Bartenschlager. The plasmid cleaved at the ScaI site was transcribed in vitro using the MEGAscript T7 kit (Ambion) according to the manufacturer's protocol. The linearized plasmid (10 μg) was introduced into Huh7 cells at 4 million cells/0.4 ml by electroporation at 270 V and 960 μF using a Gene Pulser™ (Bio-Rad, Hercules, CA). Electroporated cells were suspended at a final volume of 10 ml of culture medium. Three-milliliter aliquots of cell suspension were mixed with 7 ml of culture medium and then the cells were seeded on culture dishes (diameter: 10 cm). The culture medium was replaced with DMEM containing 10% FCS and 1 mg/ml of G418 (Nakarai Tesque) at 24 h post-transfection. The medium was exchanged weekly for fresh DMEM containing 10% FCS and 1 mg/ml G418. The remaining colonies were fixed with 4% paraformaldehyde at 4 weeks after electroporation, and the cells were stained with crystal violet.

Transient replication assay

The cDNA encoding Renilla luciferase was introduced between the AscI and PmeI sites of the plasmid pFK-I$_{389}$ neo/NS3-3'/NK5.1, in place of the neo gene. The resulting plasmid, pFK-I$_{389}$ hRL/NS3-3'/NK5.1, was cleaved with ScaI and was transcribed in vitro using a MEGAscript T7 kit (Ambion). Huh7 cells were suspended at 10 million cells/ml and the suspensions were mixed with 10 μg of in vitro-transcribed RNA at a 400-μl volume; the cells were then electroporated at 270 V and 960 μF by a Gene Pulser™ (Bio-Rad). The electroporated cells were suspended in 25 ml of culture medium and then were seeded at 1 ml/well on 12-well culture plates. Luciferase activity was measured at 4 and 48 h post-transfection using a Renilla Luciferase assay system (Promega, Madison, WI) according to the manufacturer's protocol. Luciferase activity at 4 h after electroporation was used to determine the transfection efficiency.

Generation of infectious HCV particles

The viral RNA of JFH1 was introduced into Huh7.5.1 according to the method of Wakita et al (2005). The supernatant was collected at 7 days post-transfection and used as HCV particles that are infectious in cell culture (HCVcc). The naïve Huh7.5.1 cells were transfected with siRNA of nontarget control or FKBP8-Target 1 at a concentration of 80 nM. The siRNA-treated Huh7.5.1 cells were inoculated with HCVcc at 24 h post-transfection. Infected cells and culture supernatants were harvested every day until 5 days post-infection.

Determination of FKBP8-binding proteins

MEF purification was carried out by a previously described method (Ichimura et al, 2005). The FKBP8 gene was amplified by PCR and introduced into pcDNA3.1 encoding the myc-TEV-Flag epitope tag (Ichimura et al, 2005). The resulting plasmid was transfected into 293T cells, which were then subjected to MEF purification. FKBP8-binding proteins were separated by SDS–PAGE and visualized by silver staining. The stained bands were excised, digested in gels with Lys-C, and analyzed by the direct nanoflow LC-MS/MS system (Ichimura et al, 2005).

Supplementary data

Supplementary data are available at The EMBO Journal Online (http://www.embojournal.org).

Acknowledgements

References

Aizaki H, Aoki Y, Harada T, Ishii K, Suzuki T, Nagamori S, Toda G, Matsuura Y, Miyamura T (1998) Full-length complementary DNA of hepatitis C virus genome from an infectious blood sample. Hepatology 27: 621–627

Appel N, Pietschmann T, Bartenschlager R (2005) Mutational analysis of hepatitis C virus nonstructural protein 5A: potential role of differential phosphorylation in RNA replication and identification of a genetically flexible domain. J Virol 79: 3187–3194

Boguski MS, Sikorski RS, Hieter P, Goebl M (1990) Expanding family. Nature 346: 114

Brinker A, Scheufler C, Von Der Mulbe F, Fleckenstein B, Herrmann C, Jung G, Moarefi I, Hartl FU (2002) Ligand discrimination by TPR domains. Relevance and selectivity of EEVD-recognition in Hsp70 × Hop × Hsp90 complexes. J Biol Chem 277: 19265–19275

Chadli A, Bouhouche I, Sullivan W, Stensgard B, McMahon N, Catelli MG, Toft DO (2000) Dimerization and N-terminal domain proximity underlie the function of the molecular chaperone heat shock protein 90. Proc Natl Acad Sci USA 97: 12524–12529

Cliff MJ, Harris R, Barford D, Ladbury JE, Williams MA (2006) Conformational diversity in the TPR domain-mediated interaction of protein phosphatase 5 with Hsp90. Structure 14: 415–426

Edlich F, Weiwad M, Erdmann F, Fanghanel J, Jarczowski F, Rahfeld JU, Fischer G (2005) Bcl-2 regulator FKBP38 is activated by Ca(2 +)/calmodulin. EMBO J 24: 2688–2699

Evans MJ, Rice CM, Goff SP (2004) Phosphorylation of hepatitis C virus nonstructural protein 5A modulates its protein interactions and viral RNA replication. Proc Natl Acad Sci USA 101: 13038–13043

Fischer G, Aumuller T (2003) Regulation of peptide bond cis/trans isomerization by enzyme catalysis and its implication in physiological processes. Rev Physiol Biochem Pharmacol 148: 105–150

Gao L, Aizaki H, He JW, Lai MM (2004) Interactions between viral nonstructural proteins and host protein hVAP-33 mediate the formation of hepatitis C virus RNA replication complex on lipid raft. J Virol 78: 3480–3488

—417—

Hamamoto I, Nishimune Y, Okamoto T, Aizaki H, Lee K, Mori Y, Abe T, Lai MC, Miyamura T, Moriishi K, Matsuura Y (2005) Human VAP-B is involved in HCV replication through interaction with NS5A and NS5B. *J Virol* **79:** 13473–13482

Hirano T, Kinoshita N, Morikawa K, Yanagida M (1990) Snap helix with knob and hole: essential repeats in *S. pombe* nuclear protein nuc2 + . *Cell* **60:** 319–328

Huang DC, Cory S, Strasser A (1997) Bcl-2, Bcl-XL and adenovirus protein E1B19kD are functionally equivalent in their ability to inhibit cell death. *Oncogene* **14:** 405–414

Ichimura T, Yamamura H, Sasamoto K, Tominaga Y, Taoka M, Kakiuchi K, Shinkawa T, Takahashi N, Shimada S, Isobe T (2005) 14-3-3 proteins modulate the expression of epithelial Na + channels by phosphorylation-dependent interaction with Nedd4–2 ubiquitin ligase. *J Biol Chem* **280:** 13187–13194

Inoue K, Sekiyama K, Yamada M, Watanabe T, Yasuda H, Yoshiba M (2003) Combined interferon alpha2b and cyclosporin A in the treatment of chronic hepatitis C: controlled trial. *J Gastroenterol* **38:** 567–572

Kapadia SB, Chisari FV (2005) Hepatitis C virus RNA replication is regulated by host geranylgeranylation and fatty acids. *Proc Natl Acad Sci USA* **102:** 2561–2566

Kashiwagi T, Hara K, Kohara M, Iwahashi J, Hamada N, Honda-Yoshino H, Toyoda T (2002) Promoter/origin structure of the complementary strand of hepatitis C virus genome. *J Biol Chem* **277:** 28700–28705

Koch JO, Bartenschlager R (1999) Modulation of hepatitis C virus NS5A hyperphosphorylation by nonstructural proteins NS3, NS4A, and NS4B. *J Virol* **73:** 7138–7146

Lackner T, Muller A, Konig M, Thiel HJ, Tautz N (2005) Persistence of bovine viral diarrhea virus is determined by a cellular cofactor of a viral autoprotease. *J Virol* **79:** 9746–9755

Lam E, Martin M, Wiederrecht G (1995) Isolation of a cDNA encoding a novel human FK506-binding protein homolog containing leucine zipper and tetratricopeptide repeat motifs. *Gene* **160:** 297–302

Lindenbach BD, Evans MJ, Syder AJ, Wolk B, Tellinghuisen TL, Liu CC, Maruyama T, Hynes RO, Burton DR, McKeating JA, Rice CM (2005) Complete replication of hepatitis C virus in cell culture. *Science* **309:** 623–626

Lohmann V, Korner F, Koch J, Herian U, Theilmann L, Bartenschlager R (1999) Replication of subgenomic hepatitis C virus RNAs in a hepatoma cell line. *Science* **285:** 110–113

Macdonald A, Harris M (2004) Hepatitis C virus NS5A: tales of a promiscuous protein. *J Gen Virol* **85:** 2485–2502

Maggioni C, Braakman I (2005) Synthesis and quality control of viral membrane proteins. *Curr Top Microbiol Immunol* **285:** 175–198

Manns MP, McHutchison JG, Gordon SC, Rustgi VK, Shiffman M, Reindollar R, Goodman ZD, Koury K, Ling M, Albrecht JK (2001) Peginterferon alfa-2b plus ribavirin compared with interferon alfa-2b plus ribavirin for initial treatment of chronic hepatitis C: a randomised trial. *Lancet* **358:** 958–965

Mayer MP (2005) Recruitment of Hsp70 chaperones: a crucial part of viral survival strategies. *Rev Physiol Biochem Pharmacol* **153:** 1–46

Moriishi K, Inoue S, Koura M, Amano F (1999) Inhibition of listeriolysin O-induced hemolysis by bovine lactoferrin. *Biol Pharm Bull* **22:** 1167–1172

Moriishi K, Matsuura Y (2003) Mechanisms of hepatitis C virus infection. *Antivir Chem Chemother* **14:** 285–297

Nakagawa M, Sakamoto N, Tanabe Y, Koyama T, Itsui Y, Takeda Y, Chen CH, Kakinuma S, Oooka S, Maekawa S, Enomoto N, Watanabe M (2005) Suppression of hepatitis C virus replication by cyclosporin a is mediated by blockade of cyclophilins. *Gastroenterology* **129:** 1031–1041

Neckers L (2002) Hsp90 inhibitors as novel cancer chemotherapeutic agents. *Trends Mol Med* **8:** S55–S61

Neddermann P, Clementi A, De Francesco R (1999) Hyperphosphorylation of the hepatitis C virus NS5A protein requires an active NS3 protease, NS4A, NS4B, and NS5A encoded on the same polyprotein. *J Virol* **73:** 9984–9991

Nielsen JV, Mitchelmore C, Pedersen KM, Kjaerulff KM, Finsen B, Jensen NA (2004) Fkbp8: novel isoforms, genomic organization, and characterization of a forebrain promoter in transgenic mice. *Genomics* **83:** 181–192

Niwa H, Yamamura K, Miyazaki J (1991) Efficient selection for high-expression transfectants with a novel eukaryotic vector. *Gene* **108:** 193–199

Pietschmann T, Lohmann V, Kaul A, Krieger N, Rinck G, Rutter G, Strand D, Bartenschlager R (2002) Persistent and transient replication of full-length hepatitis C virus genomes in cell culture. *J Virol* **76:** 4008–4021

Pietschmann T, Lohmann V, Rutter G, Kurpanek K, Bartenschlager R (2001) Characterization of cell lines carrying self-replicating hepatitis C virus RNAs. *J Virol* **75:** 1252–1264

Pirkl F, Fischer E, Modrow S, Buchner J (2001) Localization of the chaperone domain of FKBP52. *J Biol Chem* **276:** 37034–37041

Qing K, Hansen J, Weigel-Kelley KA, Tan M, Zhou S, Srivastava A (2001) Adeno-associated virus type 2-mediated gene transfer: role of cellular FKBP52 protein in transgene expression. *J Virol* **75:** 8968–8976

Scheufler C, Brinker A, Bourenkov G, Pegoraro S, Moroder L, Bartunik H, Hartl FU, Moarefi I (2000) Structure of TPR domain-peptide complexes: critical elements in the assembly of the Hsp70-Hsp90 multichaperone machine. *Cell* **101:** 199–210

Shirane M, Nakayama KI (2003) Inherent calcineurin inhibitor FKBP38 targets Bcl-2 to mitochondria and inhibits apoptosis. *Nat Cell Biol* **5:** 28–37

Silverstein AM, Galigniana MD, Kanelakis KC, Radanyi C, Renoir JM, Pratt WB (1999) Different regions of the immunophilin FKBP52 determine its association with the glucocorticoid receptor, hsp90, and cytoplasmic dynein. *J Biol Chem* **274:** 36980–36986

Tellinghuisen TL, Marcotrigiano J, Gorbalenya AE, Rice CM (2004) The NS5A protein of hepatitis C virus is a zinc metalloprotein. *J Biol Chem* **279:** 48576–48587

Tellinghuisen TL, Marcotrigiano J, Rice CM (2005) Structure of the zinc-binding domain of an essential component of the hepatitis C virus replicase. *Nature* **435:** 374–379

Tu H, Gao L, Shi ST, Taylor DR, Yang T, Mircheff AK, Wen Y, Gorbalenya AE, Hwang SB, Lai MM (1999) Hepatitis C virus RNA polymerase and NS5A complex with a SNARE-like protein. *Virology* **263:** 30–41

Wakita T, Pietschmann T, Kato T, Date T, Miyamoto M, Zhao Z, Murthy K, Habermann A, Krausslich HG, Mizokami M, Bartenschlager R, Liang TJ (2005) Production of infectious hepatitis C virus in tissue culture from a cloned viral genome. *Nat Med* **11:** 791–796

Wang C, Gale Jr M, Keller BC, Huang H, Brown MS, Goldstein JL, Ye J (2005) Identification of FBL2 as a geranylgeranylated cellular protein required for hepatitis C Virus RNA replication. *Mol Cell* **18:** 425–434

Wasley A, Alter MJ (2000) Epidemiology of hepatitis C: geographic differences and temporal trends. *Semin Liver Dis* **20:** 1–16

Watashi K, Hijikata M, Hosaka M, Yamaji M, Shimotohno K (2003) Cyclosporin A suppresses replication of hepatitis C virus genome in cultured hepatocytes. *Hepatology* **38:** 1282–1288

Watashi K, Ishii N, Hijikata M, Inoue D, Murata T, Miyanari Y, Shimotohno K (2005) Cyclophilin B is a functional regulator of hepatitis C virus RNA polymerase. *Mol Cell* **19:** 111–122

Waxman L, Whitney M, Pollok BA, Kuo LC, Darke PL (2001) Host cell factor requirement for hepatitis C virus enzyme maturation. *Proc Natl Acad Sci USA* **98:** 13931–13935

Wu B, Li P, Liu Y, Lou Z, Ding Y, Shu C, Ye S, Bartlam M, Shen B, Rao Z (2004) 3D structure of human FK506-binding protein 52: implications for the assembly of the glucocorticoid receptor/Hsp90/immunophilin heterocomplex. *Proc Natl Acad Sci USA* **101:** 8348–8353

Ye J, Wang C, Sumpter Jr R, Brown MS, Goldstein JL, Gale Jr M (2003) Disruption of hepatitis C virus RNA replication through inhibition of host protein geranylgeranylation. *Proc Natl Acad Sci USA* **100:** 15865–15870

Yi M, Lemon SM (2004) Adaptive mutations producing efficient replication of genotype 1a hepatitis C virus RNA in normal Huh7 cells. *J Virol* **78:** 7904–7915

Zhong J, Gastaminza P, Cheng G, Kapadia S, Kato T, Burton DR, Wieland SF, Uprichard SL, Wakita T, Chisari FV (2005) Robust hepatitis C virus infection *in vitro*. *Proc Natl Acad Sci USA* **102:** 9294–9299

ORIGINAL ARTICLE

Nucleolin is involved in interferon regulatory factor-2-dependent transcriptional activation

A Masumi[1], H Fukazawa[2], T Shimazu[3], M Yoshida[3], K Ozato[4], K Komuro[1] and K Yamaguchi[1]

[1]Department of Safety Research on Blood and Biological Products, National Institute of Infectious Diseases, Tokyo, Japan; [2]Department of Bioactive Molecules, National Institute of Infectious Diseases, Tokyo, Japan; [3]Chemical Genetics Laboratory, RIKEN, Saitama, Japan and [4]Laboratory of Molecular Growth and Regulation, National Institute of Child Health and Human Development, National Institute of Health, Bethesda, MD, USA

We have previously shown that interferon regulatory factor-2 (IRF-2) is acetylated in a cell growth-dependent manner, which enables it to contribute to the transcription of cell growth-regulated promoters. To clarify the function of acetylation of IRF-2, we investigated the proteins that associate with acetylated IRF-2. In 293T cells, the transfection of p300/CBP-associated factor (PCAF) enhanced the acetylation of IRF-2. In cells transfected with both IRF-2 and PCAF, IRF-2 associated with endogenous nucleolin, while in contrast, minimal association was observed when IRF-2 was transfected with a PCAF histone acetyl transferase (HAT) deletion mutant. In a pull-down experiment using stable transfectants, acetylation-defective mutant IRF-2 (IRF-2K75R) recruited nucleolin to a much lesser extent than wild-type IRF-2, suggesting that nucleolin preferentially associates with acetylated IRF-2. Nucleolin in the presence of PCAF enhanced IRF-2-dependent H4 promoter activity in NIH3T3 cells. Nucleolin knock-down using siRNA reduced the IRF-2/PCAF-mediated promoter activity. Chromatin immunoprecipitation analysis indicated that PCAF transfection increased nucleolin binding to IRF-2 bound to the H4 promoter. We conclude that nucleolin is recruited to acetylated IRF-2, thereby contributing to gene regulation crucial for the control of cell growth.
Oncogene (2006) 25, 5113–5124. doi:10.1038/sj.onc.1209522; published online 3 April 2006

Keywords: IRF-2; nucleolin; acetylation

Introduction

Interferon regulatory factors (IRFs) have been studied in the context of host defense and oncogenesis (Taniguchi et al., 2001) and transcriptional regulation (Schaffer et al., 1997). Interferon regulatory factor-2 (IRF-2) has generally been described as a transcriptional repressor, and is thought to function by competing with the transcriptional activator IRF-1. However, IRF-2 can act as a positive regulator for interferon stimulated response element (ISRE)-like sequences such as the promoters H4 (Vaughan et al., 1998; Xie et al., 2001), vascular adhesion molecule-1 and gp91phox (Luo and Skalnik, 1996) as well as Fas ligand (Chow et al., 2000). Biologically, IRF-2 plays an important role in cell growth regulation, and has been shown to be a potential oncogene (Yamamoto et al., 1994). A recent report indicated that IRF-2 drives megakaryocytic differentiation through regulation of the thrombopoietin receptor promoter (Stellacci et al., 2004). It has been reported that many transcription factors, such as MyoD, β-catenin, p53, Tat and CTIIA regulate specific promoters associated with the coactivators p300 and p300/CBP-associated factor (PCAF), and that this regulation leads to specific biological functions (Lakin and Jackson, 1999; Deng et al., 2000; Spilianakis et al., 2000; Polwsskaya et al., 2001; Wolf et al., 2002). Certain IRF proteins interact with other transcription factors such as TFIIB, and the coactivators p300 and PCAF (Wang et al., 1996; Yoneyama et al., 1998; Masumi et al., 1999) and these interactions lead to transcriptional activation or repression depending on the cell types involved. To clarify the regulatory functions of transcription factors, many investigators have studied the coactivators, such as p300 and PCAF.

There are many reports of the histone acetyltransferases such as PCAF, p300/CBP and GCN5 acting as co-activators (Benkirane et al., 1998; Vassilev et al., 1998; Hamamori et al., 1999; Jiang et al., 1999; Masumi et al., 1999; Schiltz et al., 1999; Harrod et al., 2000; Lau et al., 2000a,b; Li et al., 2000; Trievel et al., 2000; Yamauchi et al., 2000; Vo and Goodman, 2001; Lang and Hearing, 2003; Patel et al., 2004). A number of transcriptional factors associate with p300/CBP, originally known as the global co-activator, and with PCAF and GCN5. Recruitment of these histone acetylases is thought to alter chromatin structures, and is required as an integral part of transcriptional activation. As a result of interaction with histone acetylases, certain transcription factors become acetylated themselves, which often results in enhanced transcriptional activity (Sterner and Berger, 2000). We have previously reported that the

5114

transfection of PCAF-enhanced IRF-2-dependent *H4* promoter activity in NIH3T3 cells, (Masumi *et al.*, 1999) and that IRF-2 was acetylated by p300 and PCAF *in vivo* and *in vitro* (Masumi and Ozato, 2001), providing the first example of acetylation in the IRF family. Since then, additional IRF members IRF-3 and IRF-7, have been shown to be acetylated by p300 and PCAF, respectively, *in vivo* and *in vitro* (Caillaud *et al.*, 2002; Suhara *et al.*, 2002). Acetylation of IRF-2 leads to inhibition of histone acetylation by p300 *in vitro*, suggesting a possible mechanism for transcriptional repression by IRF-2 in U937 cells (Masumi and Ozato, 2001). In contrast, we demonstrated that acetylation of IRF-2 regulates cell growth by activation of the *H4* promoter (Masumi *et al.*, 2003). In NIH3T3 cells, IRF-2 associates with endogenous p300 and becomes acetylated, binds to an ISRE site, and activates *H4* promoter activity. Thus, we demonstrated that IRF-2 acts as repressor and activator through its acetylation. In this paper, which aimed to identify the protein that associates with acetylated IRF-2, we performed pull-down assay by using tagged a IRF-2 expression system and showed that IRF-2, acetylated by PCAF, recruits nucleolin and activates transcription. Nucleolin is reported to be a ubiquitously expressed multifunctional protein involved in ribosomal biogenesis and the regulation of nucleolar translocation of ribosomal proteins (Ginisty *et al.*, 1992; Srivastava and Pollard, 1999). Our results reveal a new function for nucleolin as an IRF-2-interacting partner and transcriptional activator.

Results

Exogenous p300/CBP-associated factor acetylates interferon regulatory factor-2 in 293T cells

We have demonstrated previously that IRF-2 acts as a transcriptional activator upon acetylation (Masumi *et al.*, 2003). To investigate IRF-2 acetylation by histone acetylases *in vivo*, flag-PCAF and flag-p300 were transfected into 293T cells with flag-IRF-2. Cells were labeled with ^{14}C-acetate 1 h before harvesting and a M2-agarose pull-down assay was performed (Figure 1). Western blot analysis of the immunoprecipitates using anti-flag M2 agarose indicated that these plasmid were expressed in 293T cells (Figure 1c). Western blot analysis of the immunoprecipitates using anti-flag M2 agarose showed that acetylation of flag-IRF-2 was enhanced by co-transfection with PCAF, and to a slightly lesser extent, by p300 (Figure 1a). The results from the incorporation of ^{14}C-acetate into p300, PCAF and IRF-2 in M2-agarose precipitates was in accordance with those seen with Western blotting (Figure 1b). The patterns of Western blotting with anti-acetyllysine antibody and the incorporation of ^{14}C-acetate in whole cell lysate transfected with any plasmid were almost similar between each lane (Figure 1a right and b right). To confirm that PCAFhistone acetyl transferase (HAT) acetylates IRF-2 in 293T cells, flag-PCAF and flag-PCAFΔHAT were transfected into 293T cells with flag-IRF-2. The pattern of Western blotting
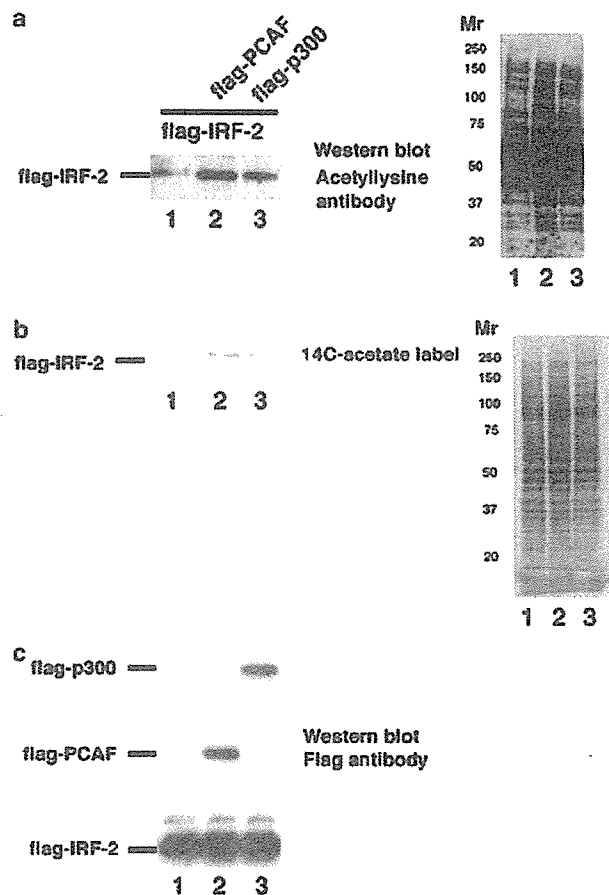

Figure 1 Interferon regulatory factor-2 (IRF-2) is acetylated by p300/CBP-associated factor (PCAF) and p300 in 293T cells. (a) 293T cells were transfected with flag-IRF-2 (1 μg) (lanes 1–3), together with flag-PCAF (1 μg) (lane 2) and flag-p300 (1 μg) (lane 3) plasmids. Of ^{14}C-acetate, 20 μCi were added 1 h before preparation of the cell lysate. Cell lysates from 293T cells were incubated with M2-agarose, and then the flag-peptide elution fraction was electrophoresed on SDS–10% PAGE and immunoblotted using an anti-acetyl lysine antibody (left). Whole lysate was electrophoresed on SDS–10% PAGE and immunoblotted with anti-acetyl lysine antibody (right) (b) Immunoblotted membranes from M2-agarose precipitates (left) and whole lysate (right) were reused for Image analysis using a Fuji BAS 2500 to visualize the ^{14}C-incorporated protein. (c) Anti-flag M2 agarose precipitates from 293T transfected cells transfected with above plasmids were electrophoresed on SDS–10% PAGE and immunoblotted with an anti-flag antibody.

for whole cell lysates did not significantly affect the results (Figure 2b). Western blot analysis of the immunoprecipitates using anti-flag M2 agarose indicated that these protein were expressed in 293T cells (Figure 2a bottom). An M2-agarose pull-down assay showed that compared to the control vector, the acetylation level of IRF-2 was increased by transfection of full-length PCAF, but not by PCAF lacking HAT activity (Figure 2a top). We detected PCAF autoacetylation as described earlier (Santos-Rosa *et al.*, 2003). These results indicate that IRF-2 acetylation is enhanced by PCAFHAT *in vivo*.
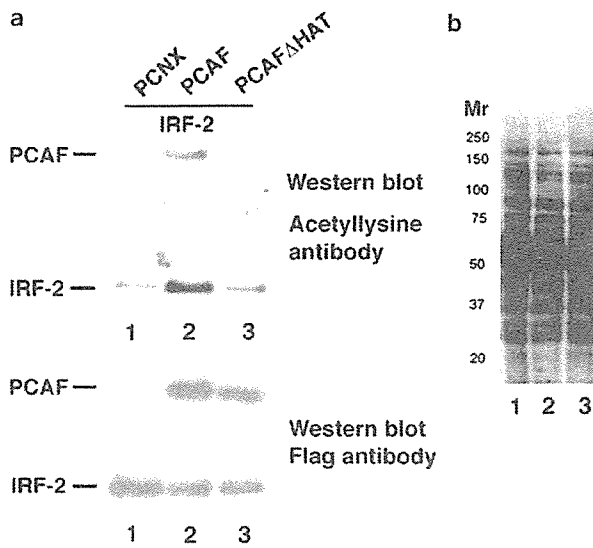
Figure 2 Western blot analysis of 293T cells transfected with interferon regulatory factor-2 (IRF-2) and p300/CBP-associated factor (PCAF). (a) 293T cells were transfected with PCNX control vector (lane 1), flag-PCAF (lane 2) and flag-PCAFΔhistone acetyl transferase (HAT) (lane 3) with flag-IRF-2. An M2-agarose-purified fraction from cell lysate was separated on SDS–10% PAGE and immunoblotted with an anti-acetyllysine (upper panel) or anti-flag antibody (bottom panel). (b) Whole cell lysates from transfected 293T cells were electrophoresed and immunoblotted with an anti-acetyllysine antibody. Full-length PCAF was auto-acetylated as shown in lane 2.

Figure 3 Coomasie blue staining pattern of the proteins co-precipitated with flag-interferon regulatory factor-2 (IRF-2). (a) 293T cells were transfected with 5 μg flag-p300/CBP-associated factor (PCAF) (lane1) alone and 5 μg flag-IRF-2 together with 5 μg flag-PCAF (lane 2). Whole cells were lyzed in a buffer B and incubated with M2-agarose, and then the flag-peptide-eluted fraction was separated on SDS–10% PAGE and the gel was stained with Coomasie brilliant blue. The two bands indicated with arrows were cut and trypsinized, and then liquid chromatography–mass spectrometry mass spectrometry (LC–MS MS) analysis was performed. Nucleolin was included in the upper band and the hsp70 family was included in the lower band. (b) 293T cells were transfected with control vector (lane 1), flag-PCAF (lane 2), flag-IRF-2 (lane 3), and flag-IRF-2 and flag-PCAF (lane 4) as described in (a). Cell lysates from 293T cells were incubated with M2-agarose, and then the flag-peptide elution fraction was prepared. Whole cells (right) and M2-agarose precipitates (left) were immunoblotted with anti-nucleolin antibody.

Interferon regulatory factor-2 recruits nucleolin in the presence of p300/CBP-associated factor

Our previous report suggested that it is the involvement of cellular proteins associated with acetylated IRF-2, which results in its transcriptional regulation (Masumi et al., 2003). To identify those proteins that associate with acetylated IRF-2, we performed an M2-agarose pull-down assay using 293T cells transfected with flag-IRF-2 and flag-PCAF. An M2-agarose-purified fraction was subjected to sodium dodecyl sulfate (SDS)–10% polyacrylamide gel electrophoresis (PAGE) and stained with Coomasie brilliant blue (Figure 3a). As shown in Figure 3a, proteins of approximately 110 and 70 kDa were observed in the immunoprecipitate from cells transfected with both flag-IRF-2 and flag-PCAF, but not in the immunoprecipitate from cells transfected with flag-PCAF alone. To identify these proteins, the bands were cut from the acrylamide gel, digested by trypsin and analysed by liquid chromatography–mass spectrometry/mass spectrometry (LC–MS/MS). Mass spectrometric analysis revealed that nucleolin was included in the 110-kDa band and that the heat shock protein 70 family was included in the 70 kDa band. As the heat shock protein 70 family is also included in the band in the PCAF-only transfected cells (Figure 3a, lane 1), we focused on nucleolin in this study. In Figure 3b, we investigated the nucleolin recruitment to IRF-2 using Western blotting. 293T cells were transfected with flag-IRF-2 in the presence or absence of flag-PCAF, and then cell lysate was incubated with anti-flag M2-agarose. The flag-peptide-eluted fraction was immunoblotted with anti-nucleolin antibody. Nucleolin expression level was not altered in any plasmid-transfected 293T cells, and nucleolin was detected most clearly in the flag-peptide-eluted fraction from cells transfected with both flag-IRF-2 and flag-PCAF (Figure 3b).

We investigated whether the histone acetylase activity of PCAF was required to recruit nucleolin to IRF-2. Flag-IRF-2 was cotransfected with flag-PCAF or flag-PCAFΔHAT into 293T cells and precipitated with M2-agarose, then analysed for the amount of recruited nucleolin by Western blotting. There was no difference of the amount of nucleolin in the lysate of 293T cells transfected with any cDNA (Figure 4a). Nucleolin was clearly identified in the affinity-purified complex from IRF-2/PCAF-transfected cells, but not in the precipitates from IRF-2/PCAFΔHAT-, IRF-2 alone-, or PCAF alone-transfected cells (Figure 4a), consistent with the
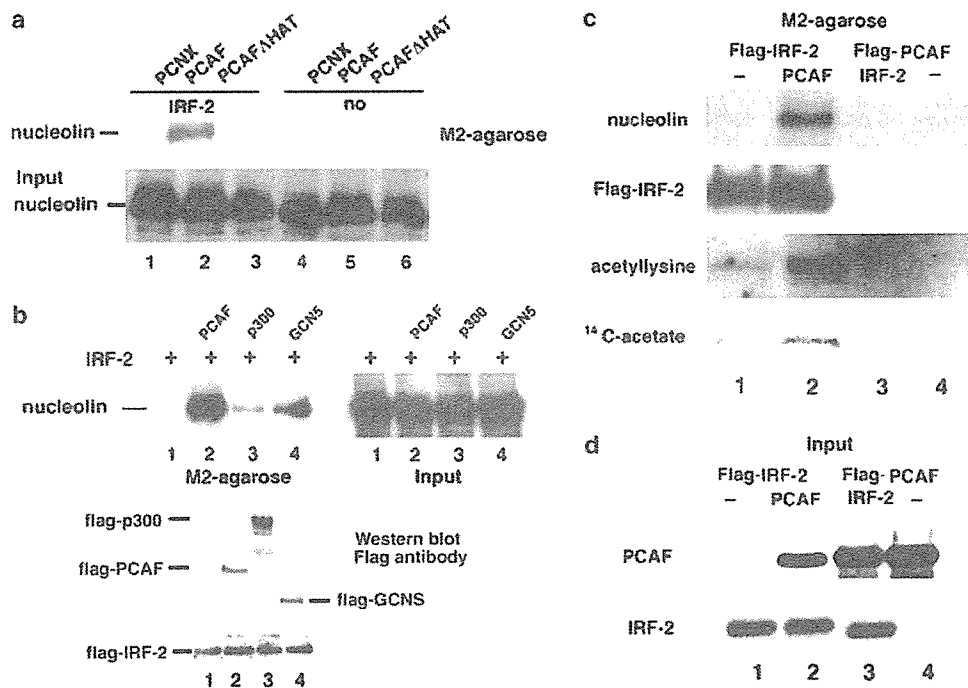
Figure 4 Nucleolin is involved in an interferon regulatory factor-2 (IRF-2)-binding complex. (a) Cell lysates from 293T cells transfected with PCNX (lanes 1 and 4), flag-p300/CBP-associated factor (PCAF) (lanes 2 and 5) and flag-PCAFΔhistone acetyl transferase (HAT) (lanes 3 and 6), flag-IRF-2 (lanes 1–3) were incubated with M2-agarose and the flag-peptide-eluted fraction was separated on a SDS–10% PAGE and immunoblotted with anti-nucleolin antibody (upper panel). Whole cell lysates from transfected 293T cells were separated on SDS–10%PAGE and immunoblotted with an anti-nucleolin antibody (bottom panel). (b) 293T cells were transfected with PCNX empty vector (lane 1), flag-PCAF (lane 2), flag-p300 (lane 3) and flag-GCN5 (lane 4) in the presence of flag-IRF-2. Cell lysate was incubated with M2-agarose and the flag-peptide-eluted fraction was separated on a SDS–10% PAGE and immunoblotted with anti-nucleolin antibody (upper left panel). Whole cell lysates from transfected 293T cells were separated on SDS–10%PAGE and immunoblotted with an anti-nucleolin antibody (upper right panel). Anti-flag M2-agarose precipitates from transfected 293T cells were immunoblotted with anti-flag antibody (bottom panel). (c) Acetylated IRF-2 preferentially recruits nucleolin in 293T cells. Flag-IRF-2 was transfected into 293T cells in the absence or presence of PCAF (without tag) (lanes 1 and 2) or flag-PCAF was transfected with or without IRF-2 (without tag) (lanes 3 and 4). ^{14}C-acetate was added to the 293T culture 1 h before harvesting. Cell lysates from 293T cells were incubated with M2-agarose and the flag-peptide fraction was electrophoresed and immunoblotted with anti-nucleolin, anti-flag, anti-acetyllysine antibodies. The membrane was reused for analysis with a BAS 2500 image analyzer to visualize ^{14}C-labeled protein. (d) Western blot analysis of PCAF and IRF-2 for whole 293T cells transfected with flag-IRF-2 (lanes 1 and 2), flag-PCAF (lanes 3 and 4), IRF-2 (lane 3) and PCAF (lane 2) was performed.

results of Figure 3b. To test whether IRF-2 recruits nucleolin in the presence of other histone acetylases, the same amount of p300 and GCN5 was transfected into 293T cells with IRF-2. As shown in Figure 4b, transfection of flag-p300 and flag-GCN5 also induced nucleolin recruitment to flag-IRF-2, although p300 recruited nucleolin to a much lesser extent compared to other histone acetylases. For comparative nucleolin recruitment to IRF-2, greater amounts of p300 may be required because of its larger molecular size. Nucleolin is not detected in the flag-peptide-eluted fraction from cell lysate transfected with only flag-IRF-2 although IRF-2 is acetylated at basal level in the absence of exogenous PCAF in 293T cells (Figures 1–4). Detectable basal acetylation level of IRF-2 does not have enough binding affinity with nucleolin in 293T cells.

To further investigate these results, PCAF without a flag-tag was transfected with flag-IRF-2 into 293T cells and then an M2-agarose pull-down assay was performed. Nucleolin was recruited more potently to

affinity-purified precipitates of both flag-IRF-2 and PCAF-transfected cells than that of the cells transfected with flag-IRF-2 alone (Figure 4c). This result is similar to that was shown in Figure 4a. In addition, we detected an increase in IRF-2 acetylation in PCAF-transfected cells, consistent with the results in Figure 2. In contrast, when flag-PCAF was cotransfected with IRF-2 (without the flag-tag) into 293T cells, nucleolin was hardly detected in the anti-flag M2-agarose precipitates (Figure 4c).

We investigated whether an increased amount of PCAF transfection led to an increase in the recruitment of nucleolin to IRF-2. Differing amounts of PCAF was transfected into 293T cells with flag-tag IRF-2 and cell lysate was incubated with anti-flag M2 agarose, and the flag-peptide-eluted fraction was then immunoblotted with anti-acetyllysine, anti-nucleolin antibodies. Acetylation of IRF-2 and nucleolin recruitment increased parallel to amount of PCAF in 293T cells (Figure 5).
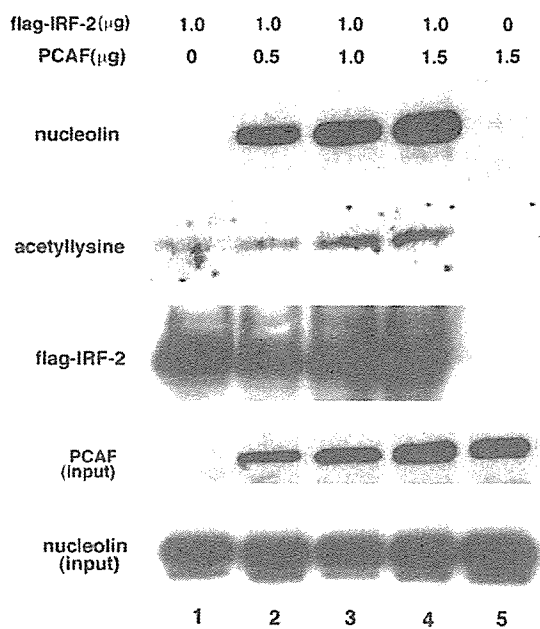
| flag-IRF-2(µg) | 1.0 | 1.0 | 1.0 | 1.0 | 0 |
| PCAF(µg) | 0 | 0.5 | 1.0 | 1.5 | 1.5 |

nucleolin

acetyllysine

flag-IRF-2

PCAF
(Input)

nucleolin
(input)

1   2   3   4   5

Figure 5 Interferon regulatory factor-2 (IRF-2) associates nucleolin in the presence of p300/CBP-associated factor (PCAF). 293T cells were transfected with several indicated amount of PCAF (lanes 1–5) and flag-IRF-2 (1 µg) (lanes 1–4). Cell lysate were incubated with anti-flag M2 agarose and flag-peptide eluted fraction were immunoblotted with anti-nucleolin, anti-acetyllysine and anti-flag antibodies. Whole cell lysate of transfected cells were immunoblot with anti-PCAF and anti-nucleolin antibodies.

We examined the localization of IRF-2 and nucleolin. HeLa cells transfected with flag-IRF-2 or a mutant flag-IRF-2K75R partially defective in acetylation (Masumi et al, 2003) with or without PCAF were fixed with paraformaldehyde and immunostained with an anti-flag antibody conjugated to cy3, and then an anti-nucleolin antibody linked with fluorescein isothiocyanate (FITC). Immunostained cells were visualized by laser scanning confocal microscopy. As shown in Figure 6a, there was no significant difference between wild-type IRF-2 and IRF-2K75R mutant-transfected HeLa cells, with nucleolin localized mainly in the nucleolus and to a lesser extent in the nucleus. Although IRF-2 localized predominantly in the nucleus, some was also localized in nucleolus. We observed that IRF-2 colocalized with nucleolin in a peri-nucleolar location. p300/CBP-associated factor transfection with both wild-type IRF-2 and K75R mutant did not change the colocalization of IRF-2 and nucleolin significantly.

To confirm if acetylatable IRF-2 recruits to nucleolin, a protein–protein interaction assay was performed using IRF-2 stably transfected cells. Cell lysates were prepared from HeLa and K562 cells stably transfected with flag-tagged wild-type IRF-2 or IRF-2K75R (Masumi et al., 2003). Lysates were incubated with anti-flag M2-agarose, and the precipitates were subjected to Western blot analysis using an anti-nucleolin antibody. In both HeLa and K562 cells, appreciable amounts of PCAF and p300 were detected (data not shown). As shown in

Figure 6b, nucleolin–IRF-2 interaction was observed in both HeLa and K562 cells that expressed wild-type IRF-2. However, in cells that expressed the K75RIRF-2 mutant (Masumi et al., 2003), the nucleolin interaction was markedly diminished. These results suggest that IRF-2 is acetylated by histone acetylases such as PCAF and p300 in these cells, and that acetylated IRF-2 preferentially associates with nucleolin.

Nucleolin transactivates interferon regulatory factor-2-enhanced H4 promoter activity
Interferon regulatory factor-2 functions as an activator for the H4 gene promoter in NIH3T3 cells (Masumi et al., 2003). To examine the functional role for nucleolin in IRF-2-dependent transcription, an *H4* gene reporter plasmid was transfected into NIH3T3 cells with IRF-2, PCAF and nucleolin. As shown in Figure 7a, transfection of nucleolin and PCAF both increased IRF-2-induced *H4* promoter activation. Co-transfection of nucleolin with PCAF further enhanced IRF-2-induced *H4* promoter activity (Figure 7a). In NIH3T3 cells, endogenous p300 may also induce IRF-2-dependent transactivation through acetylation, resulting in its interaction with nucleolin. In addition, co-transfection with HAT-deficient PCAF had no effect on nucleolin/IRF-2 activity. (Figure 7a). Co-transfection of the K75RIRF-2 mutant with PCAF/nucleolin resulted in a much lower activation of the *H4* promoter in NIH3T3 cells than with wild-type IRF-2 (Figure 7b). To examine nucleolin contribution to IRF-2-mediated *H4* promoter activation, we performed luciferase reporter assay using nucleolin small interfering RNA (siRNA). NIH3T3 cells were transfected with nucleolin siRNA to knock-down endogenous nucleolin and then transfected with IRF-2, PCAF with *H4* promoter-conjugated luciferase reporter. Compared to the control siRNA transfection, nucleolin siRNA transfection reduced the endogenous nucleolin protein in NIH3T3 cells (Figure 7d) and downregulated the IRF-2/PCAF-mediated *H4* promoter activation (Figure 7c). These results confirm that nucleolin contributes to IRF-2/PCAF-mediated transcriptional activation in NIH3T3 cells.

We have shown previously that acetylation of IRF-2 is related to cell growth (Masumi et al., 2003) and have therefore investigated whether IRF-2 is associated with nucleolin in growing NIH3T3 cells. For confocal analysis, we detected that IRF-2 and nucleolin were localized in nuclei and nucleoli in both growing and growth-arrested NIH3T3 cells. There was no significant difference between either type of NIH3T3 cell (Figure 8a). We performed a DNA affinity binding assay with biotinylated *H4* promoter oligonucleotides that had been conjugated to magnetic beads. Nuclear extracts from growing and growth-arrested cells were incubated with the beads-conjugated *H4* promoter DNA. Interferon regulatory factor-2 was detected in an eluted fraction from beads incubated with growing cell nuclear extract as reported earlier (Figure 8b) (Masumi et al., 2003). We found that while a similar level of nucleolin was detected in both growing and growth-arrested cells, H4 promoter DNA was bound to
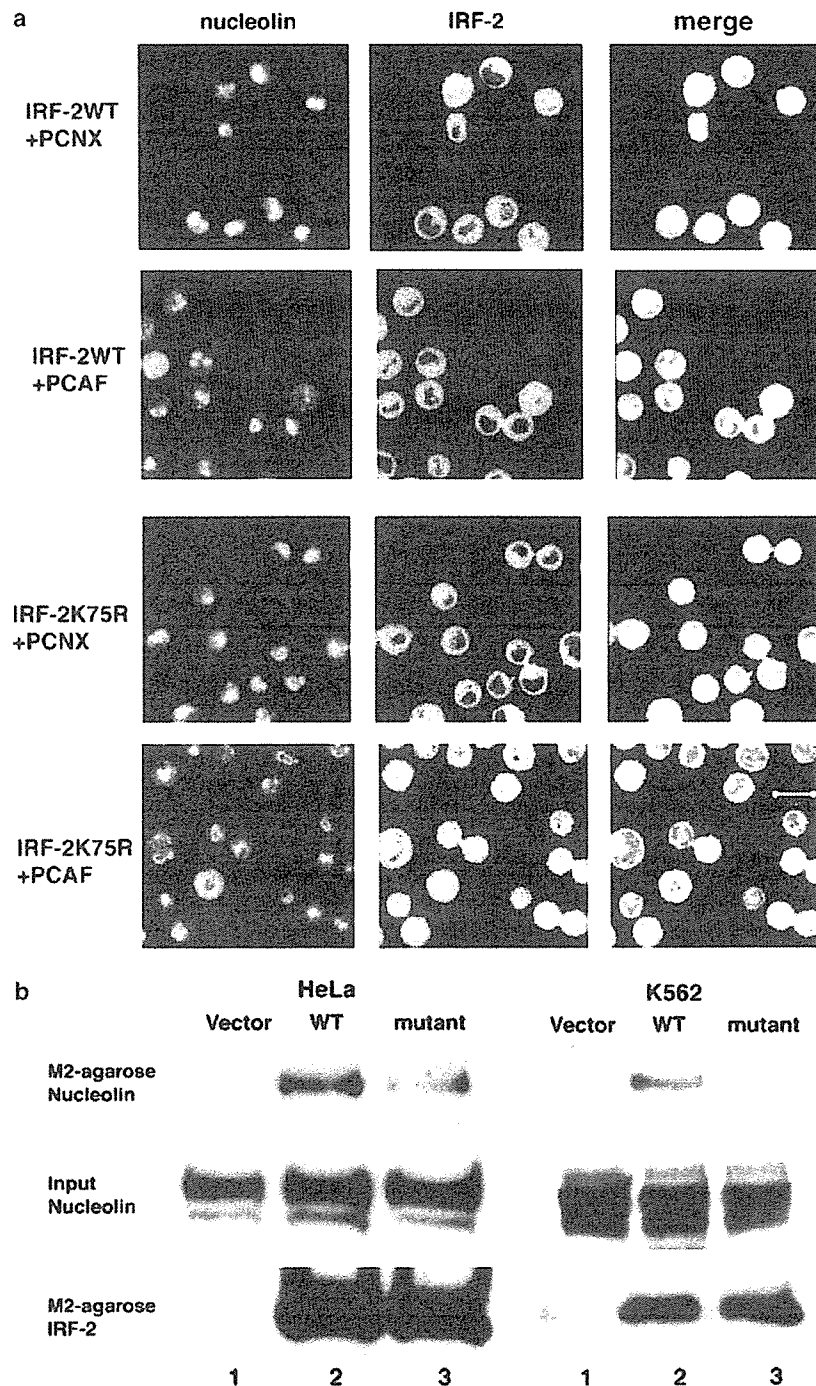
5118

a nucleolin IRF-2 merge

IRF-2WT
+PCNX

IRF-2WT
+PCAF

IRF-2K75R
+PCNX

IRF-2K75R
+PCAF

b

	HeLa			K562		
	Vector	WT	mutant	Vector	WT	mutant
M2-agarose Nucleolin						
Input Nucleolin						
M2-agarose IRF-2						

1 2 3 1 2 3

Figure 6 Interferon regulatory factor-2 (IRF-2) colocalizes and associates with nucleolin. (a) Laser scanning confocal microscopy was carried out on HeLa cells transiently transfected with flag-IRF-2 and flag-IRF-2K75R with or without p300/CBP-associated factor (PCAF). The cells were fixed with paraformaldehyde 24 h after transfection and lysed with 0.2% TritonX-100 for 10 min. Then, cells were immunocytostained with a anti-flag conjugated to Cy3 (red fluorescence) antibody for 24 h, following which, washed cells were immunostained with anti-nucleolin linked with fluorescein isothiocyanate (FITC) (green fluorescence) for 24 h. These washed cells were covered with glycerol and examined by laser scanning confocal microscopy. Colocalization of proteins results in a merging of red and green fluorescence to produce a yellow image. (b) Cell lysate from HeLa (left) and K562 (right) cells stably transfected with an empty vector (lane 1), flag-IRF-2 (lane 2) and flag-IRF-2K75R mutant (lane 3) were incubated with anti-flag M2-agarose and flag-peptide-eluted fractions were separated on SDS–10% PAGE and immunoblotted with anti-nucleolin (top) and anti-IRF-2 (bottom) antibodies. Whole cell lysates were separated on SDS–10% PAGE and immunoblotted with an anti-nucleolin antibody (middle).

—424—
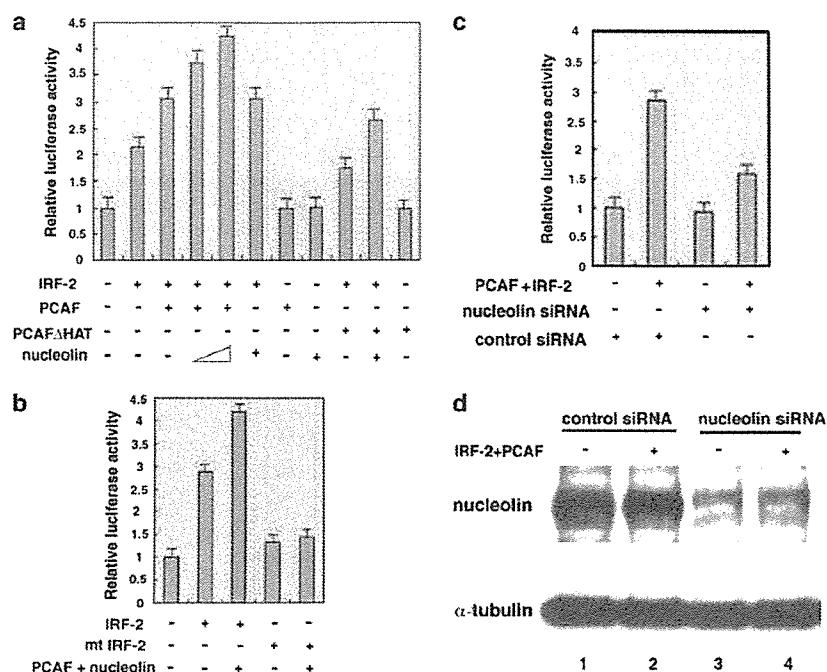
Figure 7 Nucleolin activates interferon regulatory factor-2 (IRF-2)-dependent *H4* promoter activity. (a) *H4* promoter reporter (400 ng), nucleolin (100 and 200 ng), p300/CBP-associated factor (PCAF)PCNX (100 and 200 ng) and PCAFΔhistone acetyl transferase (HAT)PCNX (200 ng) were transfected with IRF-2pcDNA3.1 (20 ng) into NIH3T3 cells. Luciferase activity was analysed 48 h after transfection. (b) Wild-type IRF-2 or mutant IRF-2 (IRF-2K75R) was transfected with nucleolin/PCAF with the *H4* promoter reporter as described in (a). Luciferase activity was analysed 48 h after transfection. The mean±s.d. from three separate experiments were calculated after normalization with TK Renilla activity. (c) Nucleolin small interfering RNA (siRNA) abrogates IRF-2/PCAF-induced *H4* promoter activation. Nucleolin siRNA was transfected into NIH3T3 cells and then PCAFPCNX and IRF-2pcDNA3.1 were transfected into NIH3T3 cells with *H4* promoter reporter. At 24 h after transfection of plasmids, luciferase activity was analysed. (d) Immunoblot analysis of NIH3T3 cell lysate transfected with nucleolin siRNA and plasmids as described in (c) using anti-nucleolin and anti-α-tubulin antibodies.

the nucleolin from growing cells only (Figure 8b). These finding are consistent with previous results, which support that the interaction of nucleolin and acetylated IRF-2 in growing cells mediate *H4* gene promoter activity (Masumi *et al.*, 2003).

From these results, it appears that the acetylation of IRF-2 rather than the change of colocalization of both factors is important for the interaction of IRF-2 and nucleolin in growing NIH3T3 cells. To confirm the association of nucleolin with IRF-2 on the *H4* promoter, chromatin immunoprecipitation analysis was performed. Chromatin was isolated from NIH3T3 cells transfected with PCAFPCNX and immunoprecipitated with anti-IRF-2 and anti-nucleolin and anti-PCAF antibodies. Immunoprecipitates were performed with polymerase chain reaction (PCR) using *H4* promoter primer as described earlier (Masumi *et al.*, 2003). As shown in Figure 8c, PCAF transfection slightly enhance the PCAF binding to *H4* promoter, however, a greater amount of nucleolin was bound to the *H4* promoter in the PCAF-transfected cells compared to control cells. In addition, a greater amount of IRF-2 was also bound to the *H4* promoter in PCAF-transfected cells compared to non-transfected cells. From these results it appears that, in NIH3T3 cells, IRF-2 and nucleolin bound the *H4* promoter more

tightly following transfection with exogenous PCAF. We conclude that nucleolin binds to acetylated IRF-2 and IRF-2/PCAF/nucleolin complexes in turn stimulate the activation of gene transcription, which drives cell growth (Figure 9).

Discussion

In this study, we have demonstrated that nucleolin acts as a positive modulator of IRF-2-dependent transcriptional activation through an association with IRF-2. Nucleolin is one of the most abundant nucleolar proteins in rapidly growing eukaryotic cells. It is multifunctional and thought to be involved in many cellular processes, including ribosome biogenesis, the processing of ribosomal RNA, mRNA stability, transcriptional regulation and cell proliferation, and it is also a downstream target of several signal transduction pathways (Ginisty *et al.*, 1992; Srivastava and Pollard, 1999). Nucleolin has been shown by proteomic analysis to associate with various proteins, such as B23, Ku80, eIF2a and the RNA binding proteins (RNP) complex (Yanagida *et al.*, 2001). Ying *et al.* (2000) reported that the interaction of nucleolin with Myb downregulated Myb transcriptional activity. Recently, Grinstein *et al.*

(2002) reported that nucleolin is a key activator of the HPV18 oncogene transcription involved in chromatin structure regulation and thus identified nuclelolin as a cellular protein with oncogenic potential. From our study we can conclude that for *H4* gene regulation by IRF-2, nucleolin acts as an oncogenic activator via

-426-
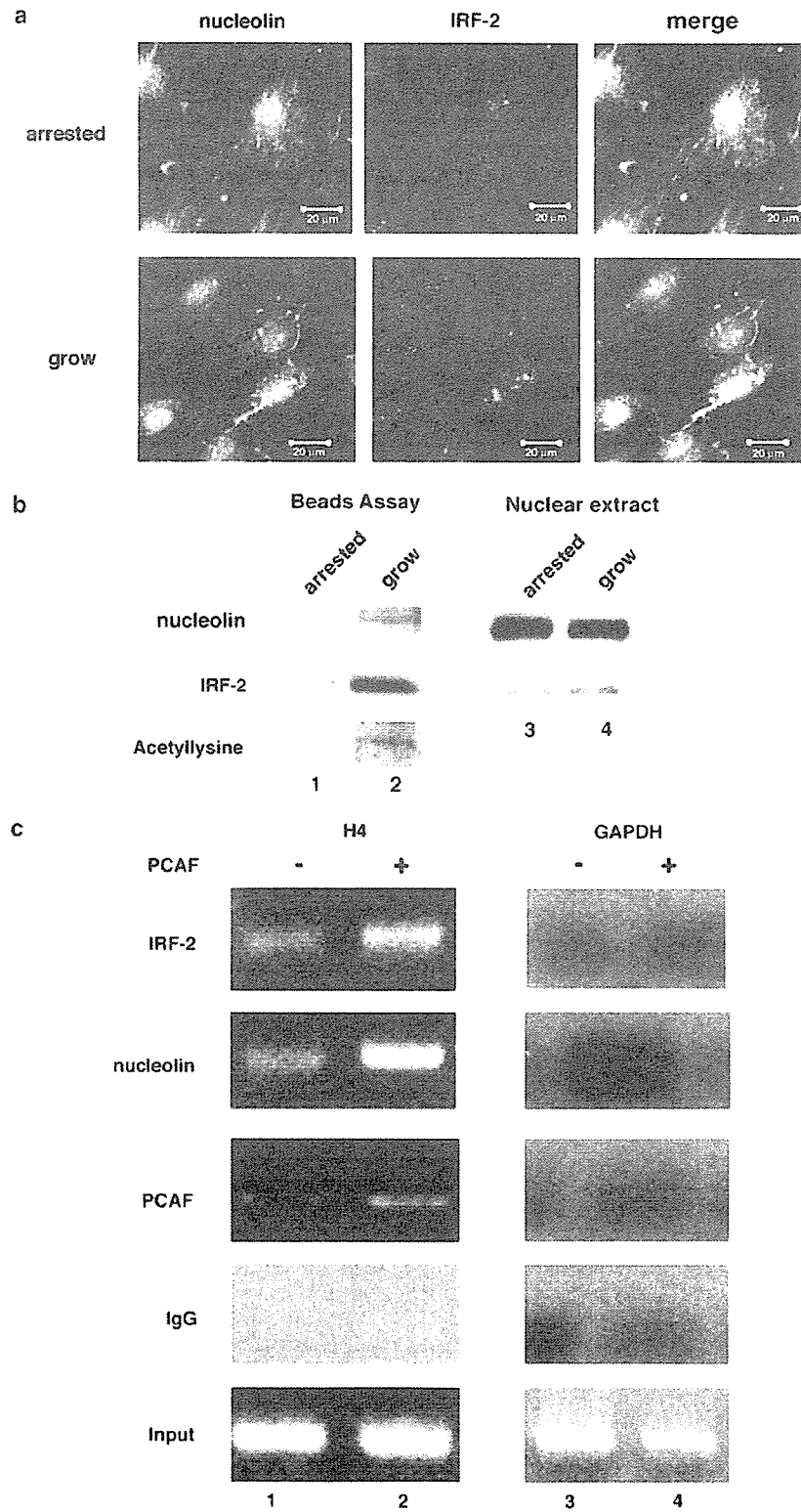
transcriptional activation, suggesting an involvement in cell growth regulation.

Previously, we demonstrated in NIH3T3 cells that lysine residues 75 and 78 in the IRF-2 DNA-binding domain are the major acetylation sites and that the IRF-2K75R mutant showed reduced *H4* promoter activity. As reported in our previous paper, p300 acts as the main acetylase for IRF-2 in NIH3T3 cells because the level of PCAF expression is so very low. However, exogenous PCAF transfection induced IRF-2-dependent transcriptional activation (Masumi *et al.*, 1999), and exogenous PCAF might induce IRF-2 acetylation in NIH3T3 cells. We also found that transfection with another histone acetylase GCN5 induced IRF-2 acetylation (data not shown) and nucleolin-IRF-2 interaction in 293T cells. We previously concluded that in NIH3T3 cells acetylated IRF-2 binds to the *H4* promoter with p300 to

Figure 9 Schematic model of the interferon regulatory factor-2 (IRF-2)-binding complex for its transcriptional regulation. p300/CBP-associated factor (PCAF) acetylates IRF-2, and acetylated IRF-2 associates with endogenous nucleolin together with PCAF. IRF-2/nucleolin/PCAF transactivates the IRF-2-specific promoter.

regulate the H4 gene (Masumi *et al.*, 2003). However, in cells with a high amount of PCAF or GCN5, IRF-2 may be acetylated by both histone acetyltransferases, as well as p300, recruit nucleolin and thus regulate specific promoters. In the *H4* promoter assay, we demonstrated that PCAF acetyltransferase activity was required for efficient activation of transcription mediated by IRF-2/nucleolin. Interferon regulatory factor-2K75R mutant partially defective acetylation reduces the activation of the *H4* promoter in the presence of PCAF/nucleolin, consistent with the results of the poor association of IRF-2K75R with nucleolin in stable transfectants.

We observed that in HeLa cells, IRF-2 colocalized with nucleolin in the peri-nucleolar region. Nucleolin has been reported to colocalize with p53 in a stress-dependent manner: it mobilizes between nucleoli, nuclei and the cytosol depending on the level of stress (Klibanov *et al.*, 2001; Daniely *et al.*, 2002). This mobilization depends on the cell condition, such as during various stage of growth or differentiation. In our confocal experiment, PCAF expression did not change the localization of either IRF-2 or nucleolin in HeLa cells. In growing and growth-arrested NIH3T3 cells, similar colocalization of nucleolin and IRF-2 is observed. p300/CBP-associated factor-mediated acetylation induces nucleolin-binding affinity to IRF-2 rather than colocalization of both factors.

Treatment with trichostatin A, a typical histone deacetylase inhibitor, enhanced both expression and acetylation of IRF-2 in IRF-2-stably transfected HeLa cells, but the association of IRF-2 with nucleolin was comparable between trichostatin A-treated and untreated HeLa cells (data not shown). Trichostatin A may affect other acetylatable transcription factors, which compete with IRF-2/nucleolin interaction. Alternatively, interaction of PCAF and p300 with IRF-2 may be required for the association of nucleolin and acetylated IRF-2. In fact, as IRF-2 binds PCAF or p300 *in vitro* and *in vivo* as reported earlier (Masumi *et al.*, 2003), acetylated IRF-2 may associate with nucleolin together with PCAF or p300. However, the nucleolin recruitment in anti-flag M2 agarose precipitate from flag-tagged PCAF-transfected cells was difficult to detect. From these results it can be concluded that nucleolin binds to IRF-2 directly, but not to PCAF. Acetylated IRF-2 could be detected at the basal level in
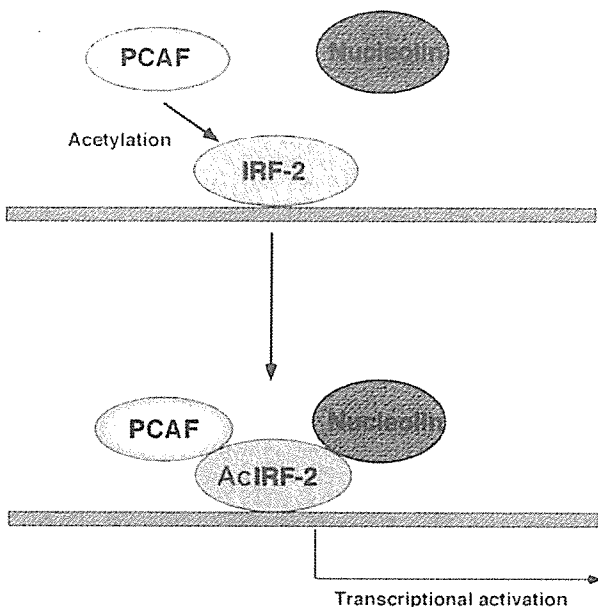
◄—————

Figure 8 Nucleolin binds *H4* promoter. (a) Laser scanning confocal microscopy was carried out on NIH3T3 cells. Growing or growth-arrested NIH3T3 cells were fixed with paraformaldehyde 24 h after transfection and lysed with 0.2% TritonX-100 for 10 min. Cells were then immunocytostained with a goat anti-interferon regulatory factor-2 (IRF-2) antibody at 4 C overnight and then immunostained with anti-goat second antibody conjugated to Alexa 488 for 2 h (green fluorescence). Following this, washed cells were immunostained with rabbit anti-nucleolin antibody and then anti-rabbit second antibody linked with Alexa 594 (red fluorescence) for 2 h. Washed cells were covered with glycerol and examined by Laser scanning confocal microscopy. Colocalization of proteins results in a merging of red and green fluorescence to produce a yellow image. (b) Nucleolin interacts with IRF-2 in growing NIH3T3 cells. Nuclear extracts were prepared from growth-arrested (lanes 1 and 3) and growing NIH3T3 cells (lanes 2 and 4), and incubated with magnetic beads conjugated to *H4* promoter. Bound materials (lanes 1 and 2) and whole nuclear extract (lanes 3 and 4) were analysed by immunoblot assay using anti-nucleolin, anti-IRF-2 and anti-acetyllysine antibodies. (c) NIH3T3 cells were transfected with p300/CBP-associated factor (PCAF) and crosslinked with 1% formaldehyde, chromatin was isolated as described under 'Materials and methods' and a chromatin immunoprecipitation assay of the *H4* promoter and glyceraldehyde-3-phosphate dehydrogenase (GAPDH) using anti-IRF-2, anti-nucleolin, anti-PCAF and rabbit immunoglobulin G (IgG) was performed. Polymerase chain reaction (PCR) quantitation was carried out as indicated under 'Materials and methods.'

5122

IRF-2-transfected 293T cells without transfection of PCAF (Figures 1–5). However, we could not detect significant nucleolin recruitment to flag-IRF-2 without transfection of PCAF. p300/CBP-associated factor transfection led to a great extent of nucleolin recruitment instead of slight increase of acetylation of IRF-2, although increasing the extent of PCAF transfection increased nucleolin recruitment and was consistent with IRF-2 acetylation (Figure 5). Acetylated IRF-2 may change its conformation and nucleolin may prefer to bind to acetylated IRF-2. Nucleolin has many acid residues such as glutamic acid and asparagic acid (Lapeyre et al., 1987). In contrast, IRF-2 has 18 lysine residues in DNA-binding domain (Masumi et al, 2003). We do not at present understand how they associate via their amino acids charge, but expect to be able to determine the binding form for both factors in the future. p300/CBP-associated factor transfection may not only enhance the acetylation but also the binding affinity of IRF-2 with nucleolin. According to the chromatin precipitation analysis, PCAF transfection enhanced nucleolin and IRF-2 binding to H4 promoter, but PCAF binding to H4 promoter was enhanced only slightly by PCAF transfection. Exogenous PCAF may contribute to the acetylation of IRF-2 rather than an association with H4 promoter.

As shown in Figure 4b, p300 transfection into cells induced much less amount of nucleolin recruitment to IRF-2 compared to PCAF transfection. Although PCAF appeared to be a slightly better IRF-2 acetylase, transfection of p300 also resulted in substantial acetylation of IRF-2 (Figure 1a). It is not clear why p300 only induced modest recruitment of nucleolin to IRF-2 (Figure 4b), despite fairly high level of IRF-2 acetylation. p300 may acetylate other proteins which compete with IRF-2 for binding to nucleolin. We are currently searching for other acetylated proteins that associate with nucleolin when PCAF or p300 is transfected.

It has been shown that p300 and PCAF interact with and acetylate HIV Tat on distinct lysine residues (Kiernan et al., 1999; Ott et al., 1999). The acetylation of the activator domain of Tat by PCAF and p300 has different biological functions for Tat, and both events increase the activation of transcription from the LTR (Ott et al., 1999, 49). In addition, Chen et al. (2002) demonstrated that acetylation of RelA at distinct sites differentially regulates various biological functions of NF-κB. Martinez-Balbas et al. (2000) showed that acetylase PCAF, and to a lesser extent CBP and p300, can acetylate E2F1 in vivo and increase its DNA-binding ability and that the acetylation status of E2F1 is affected by the histone deacetylase associated with the RB–E2F1 complex. Thus, acetylation of transcription factors leads to changes in their biological activity in terms of DNA-binding affinity, transcriptional activity, interaction with other proteins, and intracellular protein stability (Bannister and Miska, 2000). In the case of IRF-2, we demonstrated that the same sites of IRF-2 were acetylated by PCAF and p300 and that acetylated IRF-2 bound to the promoter more efficiently than non-acetylated IRF-2 in vivo as shown earlier (Masumi et al.,

2003). Acetylated and non-acetylated IRF-2 appear to bind differently to cellular proteins. Acetylated IRF-2 binds to promoters more efficiently, probably by recruiting cellular factors, such as the nucleolin identified in this study.

Barlev et al. (2001) showed that acetylated p53 binds more tightly to the transcriptional cofactors transformation/transcription domain-associated protein (TRRAP) and CREB-binding protein than non-acetylated p53, although acetylated and non-acetylated p53 bind to the p21 promoter in the same manner. Levy et al. (2004) demonstrated that acetylated β-catenin associates preferentially with Tcf4 (T-cell factor/lymphoid enhancer factor) and that co-activaion of β-catenin/Tcf by p300 is mediated in part by acetylation of β-catenin. In our study, we have confirmed that PCAF-acetylated IRF-2 forms a complex with nucleolin. Histone acetylases such as PCAF and p300 mediate IRF-2-dependent transcriptional activation through nucleolin–IRF-2 interaction. Our findings provide the biological evidence for a transcriptional regulatory mechanism which is effected via protein acetylation.

Materials and methods

Cell culture and transfection
NIH 3T3 cells were grown in Dulbecco's-modified Eagle's medium (DMEM) (Sigma, St. Louis, MI, USA) with 10% calf serum (GIBCO BRL, Rockvile, MD, USA), penicillin (100 U/ml) and streptomycin (100 μg/ml) at 37°C in 5% CO_2 and 95% air. NIH 3T3 cells were transfected with H4 reporter using lipofectamine (Invitrogen, Carlsbad, CA, USA) as described earlier (Masumi et al., 2003). For making growth-arrested NIH3T3 cells, DMEM containing 0.5% calf serum was added to growing NIH3T3 cells, and cells were cultured for 48 h. HeLa and 293T cells were grown in DMEM with 10% fetal calf serum (Sigma). 293T cells were then transfected with IRF-2pcDNA3.1, PCAFPCNX and p300pCI plasmids (Masumi et al, 1999; Masumi and Ozato, 2001) using Fugene 6 (Roche Biochemicals, Indianapolis, IN, USA). At 24–48 h after transfection, cells were lysed in a buffer B (Tris-HCl, pH 8.0, 0.1 mM ethylenediamine tetraacetic acid (EDTA), 100 mM NaCl, 0.1% NP-40), containing a protease inhibitor mix (Sigma). For some experiments, 20 μCi of ^{14}C-acetate (Amersham, Piscataway, NJ, USA) were added 1 h before preparation of the cell lysate. Cell lysates were used for an anti-flag M2-agarose pull-down assay. K562 cells were cultured in RPMI medium (Sigma) with 10% fetal calf serum. To produce stable transfectants, HeLa and K562 cells were transfected with IRF-2 or IRF-2K75R (Masumi et al., 2003) using Fugene 6 (Roche Biochemicals) and cultured for 2 weeks in the presence of 400 μg/ml G418. G418-resistant cells were pooled and lysed for preparation of cell lysate. The nucleolin plasmid was a kind gift from Dr S Murakami (Hirano et al., 2003).

Western blotting
Whole cell lysates were prepared in lysis buffer B, with the addition of a protease inhibitor cocktail (Sigma). The insoluble materials and whole cell lysates containing equal amounts of total proteins were suspended in an SDS sample buffer boiled, separated on SDS–10% PAGE, and transferred onto polyvinylidene difluoride membranes (Millipore, Bedford, MA, USA). The membranes were blocked with 5% non-fat dry milk

—428—

in a phosphate-buffered saline (PBS)-T buffer (PBS containing 0.5% Tween 20) for 1 h, incubated with anti-IRF-2 (Santa Cruz), anti-p300 (Santa Cruz), anti-acetyl lysine (New England Biology, Beverly, MA, USA) and anti-flag (Sigma) antibodies for 1 h, and washed in PBS-T. The antigen–antibody interaction was visualized by incubation in a chemiluminescent reagent (Perkin Elmer Co. Ltd) and exposure to X-ray film. Immunoblotted membranes were reused for Image analysis using a Fuji BAS 2500 (Fuji Film, Japan) to visualize ^{14}C-incorporated protein.

Affinity DNA-binding assay
The DNA affinity-binding assay was performed as described (Masumi *et al.*, 2003). Briefly, nuclear extracts (500 μg of protein) were incubated with magnetic beads conjugated to biotinylated oligonucleotide from the H4 gene. Bound materials were immunoblotted with anti-nucleolin antibody.

Chromatin immunoprecipitation
A total 1×10^7 NIH3T3 cells were crosslinked with 1% formaldehyde for 15 min at room temprature. Cells were washed with PBS and resuspended in 1 ml of lysis buffer (1% SDS, 10 mM EDTA, 50 mM Tris-HCl, pH 8.0) plus a protein inhibitor mixture (Sigma), incubated on ice for 10 min, and sonicated to an average size of 500 bp by an ultrasonic cell disruptor (Ultra 5 homogenizer, TAITEC). Aliquots (100 μl) of sonicated chromatin were diluted in 1 ml of buffer (1% Triton X-100, 2 mM EDTA, 150 mM NaCl, 20 mM Tris-HCl, pH 8) and precleared with 2 μg of sheared salmon sperm DNA and protein G-Sepharose (Invitrogen) for 2 h at 4°C. Immunoprecipitation was performed overnight at 4°C with anti-IRF-2, anti-nucleolin (Santa Cruz) anti-PCAF (UBI) and rabbit immunoglobulin G (IgG) (Sigma). A 50-μl aliquot protein G-Sepharose, and 2 μg of salmon sperm DNA were added to each immunoprecipitation and incubated for 1 h. Precipitates were washed as described earlier and samples were extracted twice with elution buffer (1% SDS, 0.1 M NaHCO₃), heated at 65°C to reverse crosslinks, and DNA fragments were purified with phenol/chloroform. A 5-μl aliquot from a total of 30 μl was used in the PCR as descried earlier (Masumi *et al.*, 2003).

Purification of interferon regulatory factor-2 precipitates and analysis of mass spectrometry
Cell lysates were prepared from 293T cells transfected with IRF-2 (flag-tag or no-tag) and PCAF (flag-tag or without tag) and incubated with 50–100 μl M2 agarose (Sigma) for 2 h with rotation. After washing with buffer B, bound proteins were eluted from M2 agarose by incubation for 5 min with 30 μl of the flag peptide (0.2 mg/ml) (Sigma) in the same buffer. Eluted protein was separated on SDS–PAGE and stained with Simply blue (Invitrogen). To identify the IRF-2-associated protein, a sliced band from the gel was digested with trypsin and peptides were analysed by LC–MS/MS using LCQ-Deca XP ion trap mass spectrometer (Thermo Electron Corp., Waltham, MA, USA).

M2-agarose pull-down assay
For the M2-agarose pull-down assay, cell lysates from the 293T transfectants were incubated with M2 agarose (Sigma) in buffer B and washed three times. Bound materials were eluted by a 0.2 mg/ml flag peptide (Sigma), resolved on SDS–12.5% PAGE, and detected by Western blotting.

Small interfering RNA experiments
NIH3T3 cells were seeded at density of 3×10^5 cells per ml onto 24-well plate. After 16 h, cells were transfected with 100 mM siRNA oligonucleotides by RNAiFect Transfection Reagent (QIAGEN, Hilden, Germany) and the siRNA-containing medium was removed after 24 h of transfection, and then IRF-2pcDNA3.1, PCAFPCNX with H4 promoter luciferase reporter were transfected into NIH3T3 cells by lipofectamine (Invitrogen). Luciferase activity was analysed 24 h after transfection with plasmids. The sequences of siRNAs used here were as follows: nucleolin, GCUUUAAAUUCCU-GUAAUATT, negative control, non-silencing Alexa Flour 488 Labeled Control siRNA (QIAGEN).

Confocal microscopy
For laser scanning focal microscopy experiments, HeLa cells were cultured in a 35 mm glass bottom dish (Matsunami Glass Ind. Ltd, Japan). At 24 h after transfection, the cells were fixed with paraformaldehyde and lysed with 0.2% TritonX-100 in order to maintain the integrity of the cellular structures. They were then stained with appropriate antibodies as follows: cells transfected with flag-IRF-2 were stained with an anti-flag M2-Cy3 (Sigma). Cells were subsequently stained with anti-nucleolin-linked FITC (Santa Cruz 'sc-8023') for 16 h. NIH3T3 cells were stained with an goat anti-IRF-2 antibody (Santa Cruz) for 16 h and then with an anti-goat second antibody linked to Alexa 488 (Molecular Probes Inc., Eugene, OR, USA) for 2 h. Cells were subsequently stained with rabbit anti-nucleolin antibody (Santa Cruz), and then anti-rabbit IgG-linked Alexa 594 (Molecular Probe Co. Ltd). Stained cells were washed with Tris-buffer saline and mounted on glass slides with a mounting medium (glycerol-PBS). Fluorescent images were collected on a Zeiss Axiovert 100 confocal microscope using a Zeiss $\times 40$ objective.

Acknowledgements

References

Bannister AJ, Miska EA. (2000). *Cell Mol life Sci* **57**: 1184–1192.
Barlev N, Liu L, Chehab N, Mansfield K, Harris K, Halazonetis T *et al.* (2001). *Mol Cell* **8**: 1243–1254.
Benkirane M, Chun RF, Xiao H, Ogryzko VV, Howard BH, Nakatani Y *et al.* (1998). *J Biol Chem* **273**: 24898–24905.

Caillaud A, Prakash A, Smith E, Masumi A, Hovanessian A, Levy D *et al.* (2002). *J Biol Chem* **277**: 49417–49421.
Chen L-F, Mu Y, Greene WC. (2002). *EMBO J* **21**: 6539–6548.
Chow W, Fang J, Yee J. (2000). *J Immunol* **164**: 3512–3518.
Daniely Y, Dimitrova DD, Borowiec JA. (2002). *Mol Cell Biol* **22**: 6014–6022.

Deng L, de la Fuente C, Fu P, Wang L, Donnelly R, Wade JD et al. (2000). Virology 277: 278–295.

Ginisty H, Sicard H, Roger B, Bouvet P. (1992). J Cell Sci 112: 761–772.

Grinstein E, Wernet P, Snijders PJF, Rosl F, Weinert I, Jia W et al. (2002). J Exp Med 196: 1067–1078.

Hamamori Y, Sartorelli V, Ogruzko V, Puri PL, Wu HY, Wang JY et al. (1999). Cell 96: 405–413.

Harrod R, Kuo YL, Tang Y, Yao Y, Vassilev A, Nakatani Y et al. (2000). J Biol Chem 275: 11852–11857.

Hirano M, Kaneko S, Yamashita T, Luo H, Qin W, Shirota Y et al. (2003). J Biol Chem 278: 5109–5115.

Jiang H, Lu H, Schiltz RL, Pise-Masison CA, Ogryzko VV, Nakatani Y et al. (1999). Mol Cell Biol 19: 8136–8145.

Kiernan RE, Vanhulle C, Schiltz L, Adam E, Xiao H, Maudoux F et al. (1999). EMBO J 18: 6106–6118.

Klibanov S, O'Hagen H, Ljungman M. (2001). J Cell Sci 114: 1867–1873.

Lakin ND, Jackson SP. (1999). Oncogene 18: 7644–7655.

Lang S, Hearing P. (2003). Oncogene 22: 2836–2841.

Lapeyre B, Bourbon H, Amalric F. (1987). Proc Natl Acad Sci 84: 1472–1476.

Lau OD, Coutney AD, Vassilev A, Marzilli LA, Cotter RJ, Nakatani Y et al. (2000a). J Biol Chem 275: 21953–21959.

Lau OD, Kundu TK, Soccio RE, Ait-Si-Ali S, Khalil EM, Vassilev A et al. (2000b). Mol Cell 3: 589–595.

Levy L, Wei Y, Labalette C, Wu Y, Renard CA, Buendia MA et al. (2004). Mol Cell Biol 24: 3404–3414.

Li J, O'Malley BW, Wong J. (2000). Mol Cell Biol 20: 2031–2042.

Luo W, Skalnik DG. (1996). J Biol Chem 271: 23445–23451.

Martinez-Balbas MA, Baner UM, Nielsen SJ, Brehm A, Kouzarides T. (2000). EMBO J 19: 662–671.

Masumi A, Ozato K. (2001). J Biol Chem 276: 20973–20980.

Masumi A, Wang I-M, Lefebvre B, Yang X-J, Nakatani Y, Ozato K. (1999). Mol Cell Biol 19: 1810–1820.

Masumi A, Yamakawa Y, Fukazawa H, Ozato K, Komuro K. (2003). J Biol Chem 278: 25401–25407.

Ott M, Schnolzer M, Gamica J, Fischle W, Emiliani S, Rackwiz HR et al. (1999). Curr Biol 9: 1489–1492.

Patel J, Du Y, Ard P, Phillips C, Carella B, Chen C et al. (2004). Mol Cell Biol 24: 10826–10834.

Polwsskaya A, Naguibneva I, Duquet A, Bengal E, Robin P, Harel-Bellan A. (2001). Mol Cell Biol 21: 5312–5320.

Santos-Rosa H, Valls1 E, Kouzarides T, Martinez-Balbas M. (2003). Nucl Acids Res 31: 4285–4292.

Schaffer BC, Paulson E, Strominger JL, Speck SH. (1997). Mol Cell Biol 17: 873–886.

Schiltz RL, Mizzen CA, Vassilev A, Cook RG, Allis CD, Nakatani Y. (1999). J Biol Chem 274: 1189–1192.

Spilianakis C, Papamatheakis J, Kretsovail A. (2000). Mol Cell Biol 20: 8489–8498.

Srivastava M, Pollard HB. (1999). FASEB J 13: 1911–1922.

Stellacci E, Testa U, Retrucci E, Benedetti E, Orsatti R, Feccia T et al. (2004). Biochem J 377: 367–378.

Sterner DE, Berger SL. (2000). Mol Cell Biol 64: 435–459.

Suhara W, Yoneyama M, Kitabayashi I, Fujita T. (2002). J Biol Chem 277: 22304–22313.

Taniguchi T, Ogasawara K, Takaoka A, Tanaka N. (2001). Annu Rev Immunol 19: 623–655.

Trievel RC, Li FY, Mamorstein R. (2000). Anal Biochem 287: 319–328.

Vassilev A, Yamauchi J, Kotani T, Prives C, Avantaggiati ML, Qin J et al. (1998). Mol Cell 2: 869–875.

Vaughan PS, van der Meijden CM, Aziz F, Harada H, Taniguchi T, van WA et al. (1998). J Biol Chem 273: 194–199.

Vo N, Goodman RH. (2001). J Biol Chem 276: 13505–13508.

Wang I-M, Blanco JCG, Tsai SY, Tsai M-J, Ozato K. (1996). Mol Cell Biol 16: 6313–6324.

Wolf D, Rodova M, Miska EA, Calvet JP, Kouzarides T. (2002). J Biol Chem 28: 25562–25567.

Xie R, van Wijnen AJ, van der Meijden C, Luong MX, Stein JL, Stein GS. (2001). J Biol Chem 276: 18624–18632.

Yamamoto H, Lamphier M, Fujita T, Taniguchi T, Harada H. (1994). Oncogene 9: 1423–1428.

Yamauchi T, Yamauchi J, Kuwata T, Tamura T, Yamashita T, Bae N et al. (2000). Proc Natl Acad Sci USA 97: 11303–11306.

Yanagida M, Shimamoto A, Nishikawa K, Furuichi Y, Takahashi N. (2001). Proteomics 1: 1390–1404.

Ying G-G, Proost P, van Damme J, Bruschi M, Introna M, Golay J. (2000). J Biol Chem 275: 4152–4158.

Yoneyama M, Suhara W, Fukuhara Y, Fukuda M, Nishida E, Fujita T. (1998). EMBO J 17: 1087–1095.

—430—

Short communication

Evaluation of 10 commercial diagnostic kits for in vitro expressed hepatitis B virus (HBV) surface antigens encoded by HBV of genotypes A to H

Toshiaki Mizuochi*, Yoshiaki Okada, Kiyoko Umemori,
Saeko Mizusawa, Kazunari Yamaguchi

*Department of Safety Research on Blood and Biological Products, National Institute of Infectious Diseases,
4-7-1 Gakuen Musashi-Murayama-shi, Tokyo 208-0011, Japan*

Abstract

Genetic variability of the hepatitis B virus (HBV) constitutes one of the major challenges for diagnosis of HBV infection. It is plausible that amino acid substitutions in the "a" determinant of the HBV surface antigen (HBsAg) that affect antigenic sites, whether originating from genetic diversity or from mutations in the HBV strain itself, will affect the sensitivity of some diagnostic kits. In fact, recent studies have indicated that some diagnostic kits had false negative results with particular HBsAg mutants. There have been, however, few substantial studies evaluating sensitivities of diagnostic kits to the HBsAg encoded by different HBV genotypes. Our recent study found that 10 diagnostic kits available in Japan were able to detect HBsAg irrespective of whether it originated from HBV genotypes A, B or C, with the latter two genotypes being the dominant species in East Asia. In this study, we extended our previous efforts by assessing the ability of diagnostic kits to detect recombinant HBsAg derived from HBV genotypes A to H. Our results demonstrated that 9 out of 10 diagnostic kits evaluated were able to detect as low as 0.2 International Units (IU)/ml HBsAg, irrespective of HBV genotype. The genotypic differences in the HBV family thus appear to have little impact on the sensitivity of currently available HBsAg diagnostic kits.
© 2006 Elsevier B.V. All rights reserved.

Keywords: HBsAg; Diagnostic kits; HBV genotype

Based on an intergroup divergence of 8% or more in the complete nucleotide sequence of approximately 3200 nucleotides, HBV has been classified into eight genotypes, designated as A to H (Okamoto et al., 1988; Norder et al., 1994; Stuyver et al., 2000; Arauz-Ruiz et al., 2002). The prevalence of specific genotypes varies geographically: genotypes A and D are widely distributed throughout the Old World, while genotypes B and C are dominant in East Asia. Furthermore, the distribution of HBV genotypes may vary over time and with population migration. It is therefore critical for diagnostic kits to be able to detect HBsAg encoded by various HBV genotypes with comparable sensitivity. Moreover, given the accumulating body of evidence that certain HBV genotypes correlate with disease features and treatment outcomes, including the severity of liver disease (Mayerat et

al., 1999; Kao et al., 2000a; Orito and Mizokami, 2003), HBe antigen seroconversion (Chu et al., 2002; Ishikawa et al., 2002), and susceptibility to anti-viral drugs (Kao et al., 2000b; Wai et al., 2002; Kao et al., 2002; Zollner et al., 2004), from a treatment perspective the specificity and sensitivity of assays for sub-typing HBV genotypes is also critical. In our previous report (Mizuochi et al., 2005), we evaluated the sensitivity of 10 diagnostic kits to serum/plasma samples containing HBsAg as well as recombinant HBsAg encoded by HBV of genotypes A, B, and C. None of the diagnostic kits examined failed to detect HBsAg of genotypes A, B, and C at the concentration of 0.2 IU/ml. Furthermore, there was no difference between naturally derived antigens, i.e. serum/plasma samples, and recombinant antigens in the outcome of assays. In the present study, we sought to extend our previous study by evaluating the same diagnostic kits for their sensitivity to HBsAg encoded by HBV of all the genotypes reported to date, i.e. A to H.

Plasma specimens of HBV Genotypes A and D were obtained from International Reagents Corporation (Kobe, Japan).

Table 1
HBsAg diagnostic kits used in this study

No.	Method	Antibody (capture/detection)
1	CLIA	Monoclonal/polyclonal
2	EIA	Monoclonal/polyclonal
3	CLIA	Monoclonal/polyclonal
4	EIA	Monoclonal/polyclonal
5	EIA	Monoclonal/monoclonal($\times$2)[a]
6	CLEIA	Polyclonal/monoclonal($\times$2)[a]
7	CLEIA	Monoclonal/monoclonal($\times$2)[a]
8	EIA	Polyclonal/monoclonal
9	CLIA	Monoclonal/monoclonal
10	CLIA	Monoclonal/monoclonal

CLIA: Chemiluminescent immunoassay; EIA: enzyme immunoassay; CLEIA: chemiluminescent enzyme immunoassay.

[a] ($\times$2): Two different monoclonal antibodies.

Table 2
HBsAg diagnostic kits used in this study listed in alphabetical order of manufacturers

Product name	Manufacturer
AxSYM HBsAg	Abbott Japan Co. Ltd.
IMx HBsAg	Abbott Japan Co. Ltd.
ARCHITECT HBsAg	Abbott Japan Co. Ltd.
PRISM HBsAg	Abbott Japan Co. Ltd.
ADVIA Centaur HBsAg Assay	Bayer Medical Ltd.
VIDAS HBsAg Ultra	bioMerieux Japan Ltd.
Monolisa HBsAg	Bio-Rad Fujirebio
Lumipulse II HBsAg	FUJIREBIO INC.
Vitros Immunodiagnostics	Ortho-Clinical
Products HBsAg Reagent Pack	Diagnostics K.K.
Elecsys HBsAg	Roche Diagnostics K.K.

Note: The order of kits in this table is not corresponding to that of Table 1.

Genotypes B and C were kindly supplied by Taiwan FDA and Japanese Red Cross, respectively. Genotypes E, F, G, and H were purchased from Teragenix Co. (Ft. Lauderdale, FL, USA). All the HBV full genomes except for genotype H were cloned into plasmids by the method described by Günther et al. (1995). All the plasmids containing HBV full genomes were able to produce HBsAg in culture supernatant by transfection into HuH-7 cells (Nakabayashi et al., 1982) with lipofectin reagent (Invitrogen Co., San Diego, CA, USA). The amount of HBsAg produced by each genotype of HBV is highly variable, depending on the promoter activity of each clone (data not shown). To minimize this variation among the genotypes, S genes were amplified by PCR from plasmids containing HBV full genomes and then cloned into the pEF6/V5-His (Invitrogen Co., San Diego, CA, USA) which has the elongation factor-1α promoter to express the inserted S genes. The S gene of genotype H was amplified with DNA extracted from the plasma sample by PCR and cloned into the same plasmid. The genotypes of all the cloned S genes were determined by sequencing. Three micrograms plasmid of each genotype were transfected into 2×10^5 HuH-7 cells/well in a six-well culture plate (Asahi Technoglass Co., Chiba, Japan) with 10 µg lipofectin reagent (Invitrogen Co., San Diego, CA, USA), and the cells were cultured at 37 °C in 5% CO_2. Culture supernatants were harvested after 3 days and stored at −20 °C until use.

The concentration of each recombinant HBsAg sample was tentatively determined by utilizing ARCHITECT HBsAg QT (Abbott Japan Co. Ltd., Chiba, Japan), which is the only quantitative assay kit approved in Japan, and expressed in IU/ml. The concentration of each sample was adjusted to 10 IU/ml with a multi-marker negative matrix (Accurun 810; BBI Co. Ltd., Boston, MA, USA). The samples were subsequently diluted to make two different concentrations (0.2 and 1.0 IU/ml). These test samples of various HBV genotypes were analyzed with 10 diagnostic kits as listed in Tables 1 and 2. Tests were performed according to the manufacturer's instruction and results were expressed as C.O.I. (cut-off index) as shown in Fig. 1A and B. All of the HBsAg samples, irrespective of their HBV genotype, tested positively in all assay kits at the concentration of 1.0 IU/ml (Fig. 1A). When the HBsAg samples at the lower concentration (0.2 IU/ml) were tested, 9 out of 10 kits gave positive

results. Only one kit (No. 8) gave negative results for the HBsAg of genotypes E and F (Fig. 1B). This sensitivity (0.2–1.0 IU/ml) approaches the satisfactory criterion according to the "Guidance for Industry" issued by the FDA or the "CTS" (Common Technical Specification) defined by the EU. Only one kit failed to give positive results for the low concentration of HBsAg (0.2 IU/ml) encoded by the HBV of genotypes E and F (Fig. 1B). The results shown in this study thus confirmed the sensitivity of currently available diagnostic kits to HBsAg encoded by HBV of genotypes A to H.

Since HBsAg genotypes F and H are genetically distant from the other six genotypes (Norder et al., 2004), concerns have been raised as to the ability of the detection of these genotypes by currently available diagnostic kits. The data in this study
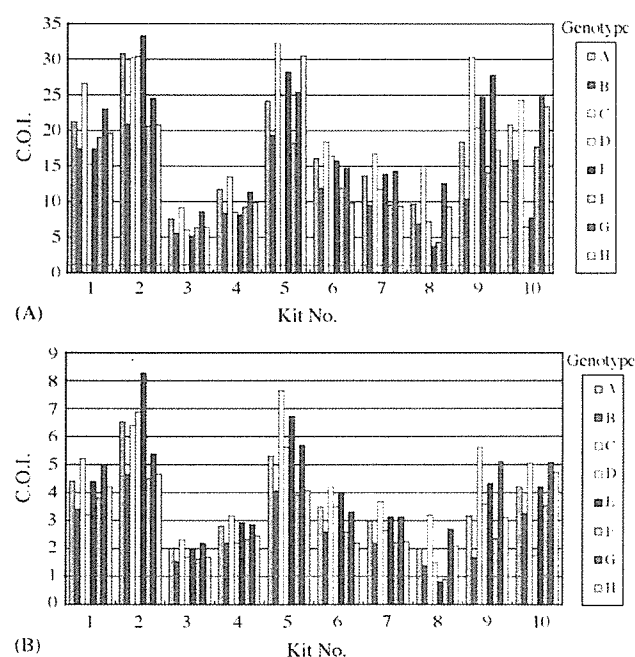

Fig. 1. Detection of recombinant HBsAg (A: 1.0 IU/ml. B: 0.2 IU/ml) derived from HBV of genotypes A to H were assayed by utilizing 10 diagnostic kits listed in Tables 1 and 2. Results were expressed as C.O.I. (cut-off index). The inserted horizontal lines indicate "C.O.I. = 1.0".

show that 9 out of 10 kits tested are capable of detecting as low as 0.2 IU/ml HBsAg including HBV genotypes F and H, alleviating this concern.

References

Arauz-Ruiz, P., Norder, H., Robertson, B.H., Magnius, L.O., 2002. Genotype H: a new Amerindian genotype of hepatitis B virus revealed in Central America. J. Gen. Virol. 83, 2059–2073.

Chu, C.J., Hussain, M., Lok, A.S., 2002. Hepatitis B virus genotype B is associated with earlier HBeAg seroconversion compared with hepatitis B virus genotype C. Gastroenterology 122, 1756–1762.

Günther, S., Li, B.-C., Miska, S., Kruger, D.H., Meisel, H., Will, H., 1995. A novel method for efficient amplification of whole hepatitis B virus genomes permits rapid functional analysis and reveals deletion mutants in immunosuppressed patients. J. Virol. 69, 5437–5444.

Ishikawa, K., Koyama, T., Masuda, T., 2002. Prevalence of HBV genotypes in asymptomatic carrier residents and their clinical characteristics during long-term follow-up: the relevance to changes in the HBeAg/anti-HBe system. Hepatol. Res. 24, 1–7.

Kao, J.H., Chen, P.J., Lai, M.Y., Chen, D.S., 2000a. Hepatitis B genotypes correlate with clinical outcomes in patients with chronic hepatitis B. Gastroenterology 118, 554–559.

Kao, J.H., Wu, N.H., Chen, P.J., Lai, M.Y., Chen, D.S., 2000b. Hepatitis B genotypes and the response to interferon therapy. J. Hepatol. 33, 998–1002.

Kao, J.H., Liu, C.J., Chen, D.S., 2002. Hepatitis B viral genotypes and lamivudine resistance. J. Hepatol. 36, 303–304.

Mayerat, C., Mantgegani, A., Frei, P.C., 1999. Does hepatitis B virus (HBV) genotype influence the clinical outcome of HBV infection? J. Viral Hepat. 6, 299–304.

Mizuochi, T., Okada, Y., Umemori, K., Mizusawa, S., Sato, S., Yamaguchi, K., 2005. Reactivity of genotypically distinct hepatitis B virus surface antigens in 10 commercial diagnostic kits available in Japan. Jpn. J. Inf. Dis. 58, 83–87.

Nakabayashi, H., Taketa, K., Miyano, K., Yamane, T., Sato, J., 1982. Growth of human hepatoma cells lines with differentiated functions in chemically defined medium. Cancer Res. 42, 3858–3863.

Norder, H., Courouce, A.M., Magnius, L.O., 1994. Complete genomes, phylogenetic relatedness, and structural proteins of six strains of the hepatitis B virus, four of which represent two new genotypes. Virology 198, 489–503.

Norder, H., Courouce, A.-M., Coursaget, P., Echevarria, J.M., Lee, S.-D., Mushahwar, I.K., Robertson, B.H., Locarnini, S., Magnius, L.O., 2004. Genetic diversity of hepatitis B virus strains derived worldwide: genotypes, subgenotypes, and HBsAg subtypes. Intervirology 47, 289–309.

Okamoto, H., Tsuda, F., Sakugawa, H., Sastrosoewignjo, R.I., Imai, M., Miyakawa, Y., Mayumi, M., 1988. Typing hepatitis B virus by homology in nucleotide sequence: comparison of surface antigen subtypes. J. Gen. Virol. 69, 2575–2583.

Orito, E., Mizokami, M., 2003. Hepatitis B virus genotypes and hepatocellular carcinoma in Japan. Intervirology 46, 408–412.

Stuyver, L., De Gendt, S., Van Geyt, C., Zoulim, F., Fried, M., Schinazi, R.F., Rossau, R., 2000. A new genotype of hepatitis B virus: complete genome and phylogenetic relatedness. J. Gen. Virol. 81, 67–74.

Wai, C.T., Chu, C.J., Hussain, M., Lok, A.S., 2002. HBV genotype B is associated with better response to interferon therapy in HBeAg(+) chronic hepatitis than genotype C. Hepatology 36, 1425–1430.

Zollner, B., Petersen, J., Puchhammer-Stockl, E., Kletzmayr, J., Sterneck, M., Fischer, L., Schroeter, R., Feucht, H.H., 2004. Viral features of lamivudine resistant hepatitis B genotypes A and D. Hepatology 39, 42–50.

Loss of Tie2 receptor compromises embryonic stem cell–derived endothelial but not hematopoietic cell survival

Isao Hamaguchi, Tohru Morisada, Masaki Azuma, Kyoko Murakami, Madoka Kuramitsu, Takuo Mizukami, Kazuyuki Ohbo, Kazunari Yamaguchi, Yuichi Oike, Daniel J. Dumont, and Toshio Suda

Tie2 is a receptor-type tyrosine kinase expressed on hematopoietic stem cells and endothelial cells. We used cultured embryonic stem (ES) cells to determine the function of Tie2 during early vascular development and hematopoiesis. Upon differentiation, the ES cell–derived Tie2$^+$Flk1$^+$ fraction was enriched for hematopoietic and endothelial progenitor cells. To investigate lymphatic differentiation, we used a monoclonal antibody against LYVE-1 and found that LYVE-1$^+$ cells derived from Tie2$^+$Flk1$^+$ cells possessed various characteristics of lymphatic endothelial cells. To determine whether Tie2 played a role in this process, we analyzed differentiation of Tie2$^{-/-}$ ES cells. Although the initial numbers of LYVE-1$^+$ and PECAM-1$^+$ cells derived from Tie2$^{-/-}$ cells did not vary significantly, the number of both decreased dramatically upon extended culturing. Such decreases were rescued by treatment with a caspase inhibitor, suggesting that reductions were due to apoptosis as a consequence of a lack of Tie2 signaling. Interestingly, Tie2$^{-/-}$ ES cells did not show measurable defects in development of the hematopoietic system, suggesting that Tie2 is not essential for hematopoietic cell development. (Blood. 2006;107:1207-1213)

© 2006 by The American Society of Hematology

Introduction

A close cell lineage relationship between hematopoietic and endothelial cells has long been recognized.[1,2] During embryogenesis, both cell types emerge in the yolk sac, and primitive erythrocytes differentiate juxtaposed to endothelial precursors by embryonic day 7.5 (E7.5).[3] In the mouse embryo, Tie2$^+$ cells in the aorta-gonad-mesonephros (AGM) region generate both blood and endothelial cells.[4] From studies of embryonic stem (ES) cell differentiation, vascular endothelial growth factor (VEGF)–responsive bipotent precursors of hematopoietic and endothelial cells, known as hemangioblasts, have been identified.[5] Hemangioblast-derived endothelial cells form vascular vessels through vasculogenesis and angiogenesis. Lymphatic development starts when a subset of vascular endothelial cells of the cardinal vein commit to a lymphatic lineage and sprout to form the primary lymph sacs at around E9 or 10.[6,7] Mouse molecular genetic experiments indicate that Prox-1 (a homeobox transcription factor) and the VEGF receptor 3 (VEGFR-3) are crucial for the commitment of endothelial cells to a lymphatic lineage.[8-10] Since lymphatic vessel–specific molecules are being identified, the molecular mechanisms underlying development of lymphatic cells as well as vascular and hematopoietic cells can now be analyzed.

Many studies report that expression of Flk1 is crucial for early establishment of endothelial and hematopoietic lineages and perhaps for their common progenitor.[5,11,12] Flk1 encodes a receptor tyrosine kinase for the vascular endothelial growth factor family of ligands.[13] Single Flk1$^+$ cells from embryoid bodies can give rise to blast colonies (blast lymphocyte colony-forming cells [BL-CFCs]), which produce both hematopoietic and endothelial cells in vitro.[5] Loss of Flk1 in mice results in selective defects in generating both blood and blood-vessel endothelial cells (BECs).[11] In addition to Flk1, Flt1 and Tie2 tyrosine kinases are also expressed in immature hematopoietic cells and BECs.[14-17]

The expression pattern of Tie2 suggests a function in both vascular endothelial and hematopoietic cells. Recently we determined the function of Ang1/Tie2 signaling, which maintains long-term repopulating hematopoietic stem cells in the bone marrow niche, suggesting that Tie2 signaling is crucial for adult bone marrow hematopoiesis.[18] In the mouse vitelline artery at E9.5, Tie2$^+$ hematopoietic cells aggregate and adhere to endothelial cells.[19] In vitro culture of Tie2$^+$ cells isolated from the AGM region generates both blood and endothelial cells.[4] In fetal liver, the Tie2$^+$ fraction contains an enriched fraction of long-term repopulating cells.[20] Based on these findings, Tie2 signaling was thought to regulate embryonic development and differentiation of hematopoietic cells. However, more recently, Puri and Berstein have demonstrated that Tie2 is dispensable for embryonic hematopoiesis using ES cell mouse chimeras.[21] This finding suggests that Tie2 function in developmental hematopoiesis differs from its role in bone marrow hematopoiesis.